



Review

UAV-based deep learning applications for automated inspection of civil infrastructure

Chen Lyu ^{a,*}, Shaoqian Lin ^a, Angus Lynch ^a, Yang Zou ^b, Minas Liarokapis ^a^a New Dexterity Research Group, Department of Mechanical and Mechatronics Engineering, The University of Auckland, Auckland 1010, New Zealand^b Department of Civil and Environmental Engineering, The University of Auckland, Auckland 1010, New Zealand

ARTICLE INFO

Keywords:

Systematic literature review
 Civil infrastructure
 Defect detection
 Unmanned aerial vehicles (UAVs)
 Deep learning

ABSTRACT

Modern technologies such as Unmanned Aerial Vehicle (UAV)-based inspection and deep learning (DL) algorithms introduce new opportunities and challenges in Civil Engineering. To better facilitate the adoption and advancement of UAV-based detection technologies, this paper conducts a systematic literature review on a plethora of articles and performs a comprehensive investigation and comparison across four different topics: (1) investigating the technical specifications of currently utilized UAV platforms and of the employed on-board sensors, (2) summarizing the categories of inspected infrastructure and the corresponding defects, (3) collecting publicly available datasets established on infrastructure defects, (4) illustrating and comparing DL algorithms designed for defect detection. Based on the analysis of collected related work, challenges hindering the development of UAV-based infrastructure inspection, solutions, and potential future opportunities are proposed. This review is aimed at assisting researchers and practitioners to accelerate progress toward more efficient and safe autonomous UAV-based structural inspection in civil engineering.

1. Introduction

Civil infrastructure constitutes the backbone of modern society, encompassing an array of structures that facilitate economic development and societal well-being [1]. Recent decades have witnessed a significant increase in civil infrastructure construction, emphasizing the need for robust periodic inspection methods. Environmental factors and excessive loading can accelerate structural deterioration, potentially leading to critical failures if unaddressed [2]. This underscores the importance of enhancing inspection techniques to ensure infrastructure longevity and safety. As shown in Fig. 1, a bridge called Morandi Bridge that serves as a transportation hub in Italy encountered a catastrophic failure of an over 200-m collapse causing 43 deaths due to poor maintenance on August 14, 2018 [3]. The collapse of the Morandi Bridge had far-reaching consequences beyond the immediate loss of life. It severely disrupted regional transportation networks and resulted in substantial economic losses, highlighting the critical importance of timely infrastructure maintenance [4]. Therefore, periodic and timely inspection of civil infrastructure plays a key role in subsequent maintenance and reducing risk of the occurrence of accidents.

Nowadays, modern civil infrastructure projects are increasingly

complex and expansive, often extending into challenging environments such as urban skylines, coastal areas, and mountainous regions. This trend has led to the development of structures with components that are difficult or hazardous for human inspectors to access. Traditional manual inspection methods for these infrastructure are time-consuming, labor-intensive, and often inadequate for the scale and complexity of modern structures [5].

Consequently, there is a growing demand for innovative inspection methods that can ensure the safety and integrity of these critical assets without compromising human safety or operational efficiency. To address these challenges, Unmanned Aerial Vehicles (UAVs) equipped with advanced sensors have emerged as a promising solution for infrastructure inspection, particularly in hard-to-reach areas [6]. As shown in Fig. 2, the integration of UAVs and deep learning (DL) algorithms presents a promising solution to these challenges, offering a more efficient and accurate approach to infrastructure defect detection. Deep learning, particularly in the field of computer vision, has shown remarkable potential for automating the inspection process. Breakthrough models such as AlexNet [7] and You Only Look Once (YOLO) [8] have demonstrated high accuracy and efficiency in image analysis tasks. When combined with UAV technology, these deep learning models can process the vast

* Corresponding author.

E-mail address: clv301@aucklanduni.ac.nz (C. Lyu).



Fig. 1. Collapse of the Morandi Bridge in Italy [3].

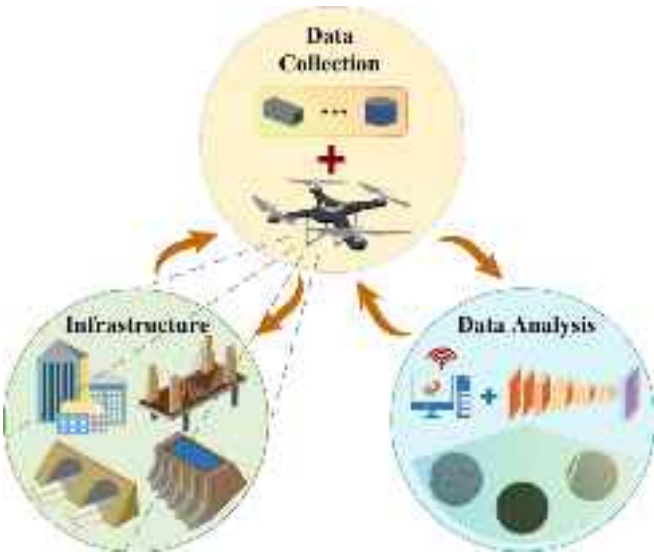


Fig. 2. Flowchart of UAV-based Automated Inspection.

amount of visual data collected during aerial inspections, enabling rapid and precise identification of structural defects [9]. This synergistic integration of UAVs and deep learning is capable of addressing the limitations of manual methods while enhancing the overall efficiency of defect detection processes.

Despite the growing application of UAV technology in infrastructure inspection, several significant challenges remain unresolved. UAV operational limitations, such as restricted flight endurance (typically 20–30 min), susceptibility to adverse weather conditions, and flight difficulties caused by GPS-denied environments, continue to impede widespread implementation [10]. Additionally, the lack of public datasets and annotation protocols for infrastructure defects creates obstacles for developing robust deep learning models. For instance, what constitutes a “severe” crack varies significantly across research studies, hindering model transferability. Furthermore, existing deep learning algorithms still struggle with detecting small-scale defects or operating effectively in low-light conditions, which are common scenarios in infrastructure inspection [11].

The potential of UAV technology has resulted in increasing number of review papers focusing on UAV-based infrastructure inspection in recent years. However, existing literature reviews exhibit limitations. Many focus narrowly on specific infrastructure types, such as powerlines [12], pavements [13], photovoltaic modules [14], or bridges [15]. While these specialized reviews provide depth in their respective domains, they fail to capture the broader technological ecosystem

necessary for comprehensive infrastructure inspection. Other reviews, while broader in scope, lack sufficient depth in critical areas. For example, Ranyal et al. [16] investigated smart sensing technology (smartphone, UAV, ground robot) applied in road condition monitoring but provided insufficient analysis of UAV capabilities and limitations. Similarly, Azimi et al. [17] reviewed structural damage detection at a general data level without adequately addressing the specific challenges of UAV-based data acquisition and processing. Additionally, Ferraris et al. [18] summarized computer vision applications in structural health monitoring but lacked focus on the integration of UAVs with these techniques. Likewise, Cha et al. [19] provided a comprehensive review of deep learning in structural monitoring but offered limited insights into the integration of various UAV platforms, sensors, deep learning algorithms, and infrastructure types.

A significant gap in current literature is the absence of comprehensive reviews that thoroughly integrate the four interdisciplinary aspects essential for effective UAV-based inspection: (1) UAV platforms and sensor technologies, (2) infrastructure types and defect categories, (3) specialized public datasets, and (4) adapted deep learning algorithms. Additionally, existing reviews have inadequately addressed emerging sensor technologies beyond visual cameras, such as Ground Penetrating Radar (GPR), ultrasonic sensors, Infrared Thermography (IRT), and Light Detection and Ranging (LiDAR), which expand UAV inspection capabilities to subsurface and internal defects. The comparative analysis of state-of-the-art deep learning algorithms specifically optimized for UAV-acquired data remains underdeveloped in current literature.

Therefore, this review paper uniquely addresses these gaps by systematically analyzing and integrating all four crucial aspects of UAV-based infrastructure inspection powered by deep learning. We focus particularly on how state-of-the-art deep learning algorithms can be integrated with UAV technology to enhance the precision and efficiency of infrastructure inspections. This review aims to provide directions for the development of UAV-based automated inspection of civil infrastructure by systematically and comprehensively analyzing existing research covering the following areas: 1) applications of UAVs and on-board sensors in terms of defect detection, 2) comparison of various prevalent open-source datasets and data analysis algorithms presently used for inspection tasks, 3) discussing current barriers limiting further development of UAV-based inspection. Through this comprehensive review, we aim to offer valuable insights to researchers and practitioners, promoting the widespread application of UAV technology on infrastructure inspection and driving future research and innovation in the field.

This paper is organized as follows. **Section 2** describes the methodology used for searching and screening related studies. **Section 3** summarizes and compares types of infrastructures and damages inspected by UAVs, UAV platforms and on-board sensors, open-source datasets and DL-based data analysis algorithms. **Section 4** discusses challenges and gaps connected with UAV-related inspection technology and outlines future research directions. Finally, **Section 5** concludes this review.

2. Methodology

This paper is constructed based on Systematic Literature Review (SLR) for a comprehensive, focused, and efficient research of previous related papers. In this review, we followed the Preferred Reporting Items for Systematic Reviews and Meta-Analyses (PRISMA) [20] which is a commonly used instruction to implement SLR for the improvement of review quality [21]. According to PRISMA, four procedures were implemented to select objective papers based on previous research. The four steps are summarized as follows: questions of research, collection of papers, screening of papers, analysis of papers. **Fig. 3** shows the process of systematic literature review conducted in this study.

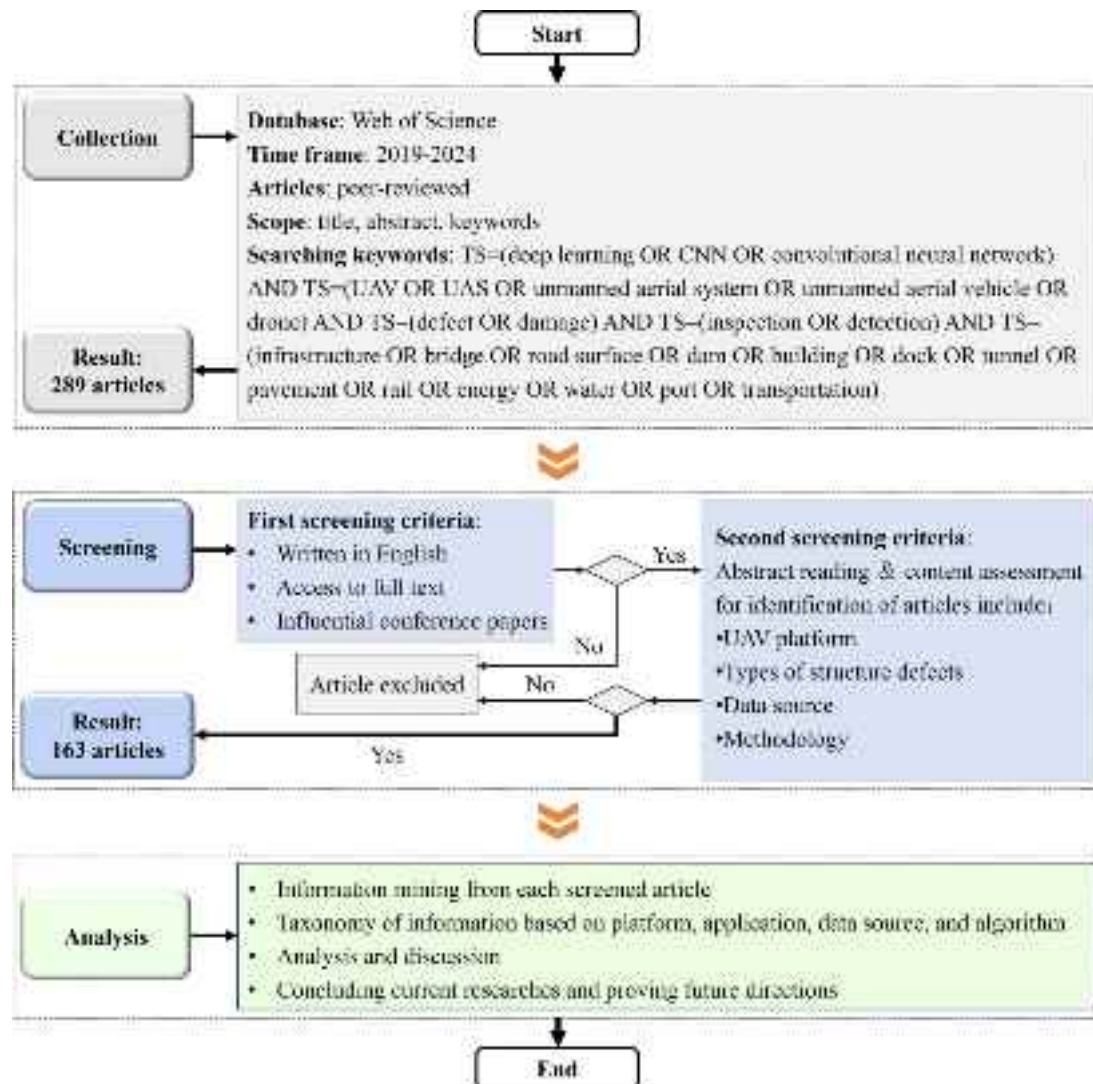


Fig. 3. Flow chart of the employed methodology.

2.1. Questions of research

To ensure the review is comprehensive and addresses the key aspects of UAV-based infrastructure inspection, we formulated specific research questions at the outset. These questions guided the entire review process and facilitated focus on the most relevant aspects of the literature. The main research questions were:

- What infrastructure types and categories of defects are currently inspected?
- What UAV platforms and on-board sensors are best utilized and what datasets are available to be used in infrastructure inspection?
- What deep learning algorithms show promise in infrastructure inspection?
- What are the challenges and gaps associated with UAV-based deep learning applications in infrastructure inspection?

According to above-mentioned research questions, a deep investigation of the state of the art was completed and was elaborated in the following subsections.

2.2. Collection of papers

This section illustrated searching process of previous studies for this

review, specific steps are:

- Database: Web of Science, which was chosen as the searching engine due to its vast collection of high-impact articles.
- Scope: Collect the most important papers. Only peer reviewed journal papers and conference papers from top tier international conferences were included.
- Time range: 2019–2024. Time frame was set in order to investigate the newest trend of computer vision technology in infrastructure inspection considering its fast and continuous updates and advancements.
- Keywords: keywords used in this review to restrict searching scope were: TS = (deep learning OR CNN OR convolutional neural network) AND TS = (UAV OR UAS OR unmanned aerial system OR unmanned aerial vehicle OR drone) AND TS = (defect OR damage) AND TS = (inspection OR detection) AND TS = (infrastructure OR bridge OR road surface OR dam OR building OR dock OR tunnel OR pavement OR rail OR energy OR water OR port OR transportation). In this case, keywords can be concluded as 4 parts based on previous predefined questions: method, platform, task, and application. Convolutional neural network (CNN) is the most frequently applied neural network in object detection algorithms, thus “convolutional neural network” and “CNN” were also considered as keywords for supplement of “deep learning”. The categories of different types of

civil infrastructure were applied for a broad and representative searching similar to that proposed by [21]. Then Boolean operators (i.e., AND, OR, and NOT) were referred to combine these keywords for more targeted collection of papers.

After the above searching strategy, 289 articles were identified in total and remained for further screening.

2.3. Screening of papers

Further screening of collected papers is necessary to guarantee papers are topic-related. This section illustrates a two-step screening progress by defining exclusion for each paper. The first-step screening include:

- Papers that were written in English.
- Papers with full access.
- Papers from influential conferences in the field.

After preliminary screening, 217 papers were selected for further exclusion. The second step was to evaluate whether these papers meet with the following eligibility by abstract reading and content assessment:

- Do the authors utilize UAV?
- Do the authors detect at least one type of infrastructure defects?
- Do the authors discuss the acquisition of data?
- Do the authors employ deep learning techniques?

Through the two-step selection, 163 papers were retrieved as a result. For reference of professionalism and relevance of journals to researchers from diverse background, journals with at least 2 papers published based on the retrieval result of this review were summarized as shown in **Table 1**. Among these Journals, Automation in Construction, Remote Sensing, and Sensors draw the most attention when it comes to infrastructure inspection.

2.4. Analysis of papers

The 163 screened papers were analyzed by thoroughly content reading and information was extracted with regard to topic of UAV platforms, sensors, datasets, defects, infrastructures, and algorithms. More specifically, the extracted information from the analysis can be summarized as follows:

- Classifications of inspected infrastructure and defects.
- UAV and mounted sensors (e.g., types and specifications).
- Datasets used for model training and testing (e.g., sources and types).
- Current DL algorithms applied for data analysis.

Each of the above topics will be precisely discussed in the next section.

3. Content analysis on UAV-assisted civil structure inspection

The overall process of civil infrastructure surveillance includes data collection platforms, detected objects, datasets used for training and testing, and applied algorithms. This section illustrates analysis results of retrieved papers based on the four main topics, specific analysis are discussed in the following subsections.

3.1. UAV platform and on-board sensors

The choice of UAV platforms, on-board sensors and their parameters is critical for identifying various types of infrastructure defects. This section summarizes the retrieved papers that discussed specific

Table 1
Journals in which the shortlisted papers were published.

| Journal | Category | Count |
|---|--------------------------------|-------|
| Automation in Construction | Civil Engineering | 13 |
| Remote Sensing | Remote Sensing | 12 |
| Sensors | Instruments & Instrumentation | 11 |
| IEEE Access | Computer Science | 7 |
| IEEE Transactions on Instrumentation and Measurement | Instruments & Instrumentation | 7 |
| Applied Sciences-Basel | Engineering, Multidisciplinary | 6 |
| Structural Control & Health Monitoring | Civil Engineering | 6 |
| Drones | Remote Sensing | 5 |
| Computer-aided Civil and Infrastructure Engineering | Civil Engineering | 4 |
| Energies | Energy & Fuels | 4 |
| Journal of Building Engineering | Civil Engineering | 3 |
| Journal of Computing in Civil Engineering | Civil Engineering | 3 |
| Structural Health Monitoring - An International Journal | Instruments & Instrumentation | 3 |
| Advanced Engineering Informatics | Artificial Intelligence | 2 |
| Applied Geomatics | Remote Sensing | 2 |
| Buildings | Civil Engineering | 2 |
| Earthquake Engineering and Engineering Vibration | Civil Engineering | 2 |
| Engineering Applications of Artificial Intelligence | Artificial Intelligence | 2 |
| Frontiers in Built Environment | Civil Engineering | 2 |
| IEEE Internet of Things Journal | Computer Science | 2 |
| International Journal of Pavement Engineering | Civil Engineering | 2 |
| Journal of Civil Structural Health Monitoring | Civil Engineering | 2 |
| Journal of Performance of Constructed Facilities | Civil Engineering | 2 |
| Neural Computing & Applications | Computer Science | 2 |
| Structures | Civil Engineering | 2 |

platforms and applied sensing devices, providing references for readers in their selection of UAVs and on-board sensors for various infrastructure inspection tasks.

3.1.1. UAV platform

Out of retrieved papers, 88 studies reported detailed description of applied UAVs. **Fig. 4** presents UAV types applied in reviewed studies and respective proportions of each type. As shown in **Fig. 4**, UAVs commonly used in infrastructure inspection can be categorized into 2 types which are fixed-wing UAV and rotary-wing UAV. Two papers in total were found that focusing on employing a fixed-wing UAV for data collection [22,23]. In study [23], it suggests that fixed-wing UAVs, compared to rotary-wing UAVs, offer higher flight speeds and longer endurance, making them suitable for covering long-distance linear areas such as highways. Additionally, fixed-wing UAVs are more stable under windy conditions than rotary-wing UAVs.

The mainstream inspection platforms are rotary-wing UAVs, which are categorized as quadcopters, hexacopters, and octocopters based on rotor quantities. This is because rotary-wing UAVs are more flexible, capable of vertical takeoff and landing, making them suitable for inspecting complex structures such as the undersides of bridges, building facades, and tunnels [24]. Their hovering capability also allows for close-range, high-precision observation of specific local structures. Among the previous studies, 89 % studies applied quadcopters for data collection, model training, or field test. Besides, studies [25–27] utilized hexacopter as a way for inspection and study [28] focused on application of octocopter. Rotary-wing UAVs can be further classified into customized UAVs and commercial UAVs, 78 studies mentioned utilizing commercial UAVs and only 10 studies aimed at customizing their own UAVs. In summary, quadcopters draw the most interests in field of infrastructure inspection.

Table 2 further summarizes the parameters and applications of

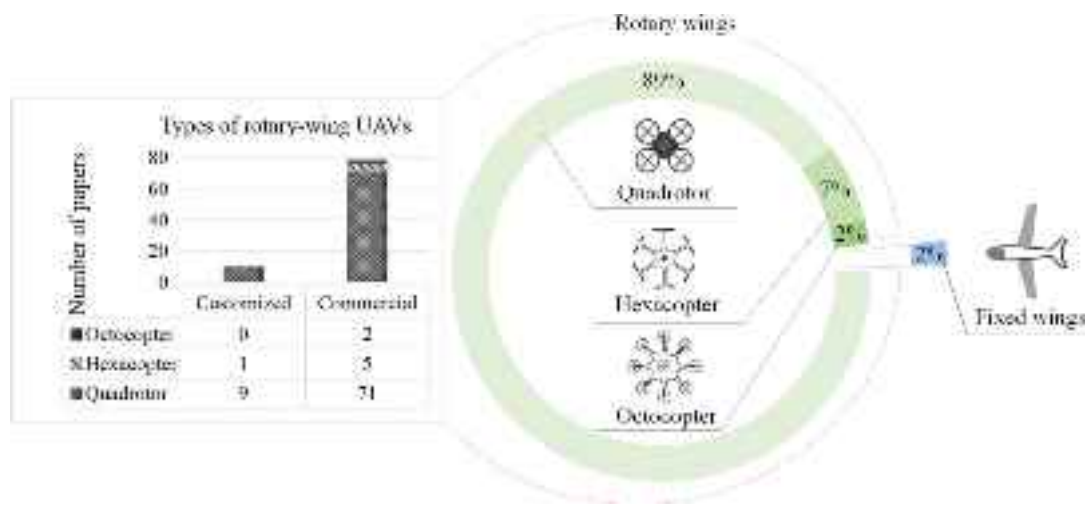


Fig. 4. Types of UAV platforms applied.

Table 2
Specifications and applications of the employed rotary-wing UAVs.

| Type | Classification | Platform | Max Flight Time (min) | Inspection Distance (m) | On-board Sensors | Applications |
|------------|----------------|----------------------------|-----------------------|-------------------------|--------------------------|---|
| Commercial | Quadrocopter | DJI Air 2S | 31 | 50 | Digital camera | Applying UAV and DL for road surface damage detection. [32] |
| | | DJI Inspire 1 | 18 | – | Digital camera | UAV image-based transmission line damper defect detection. [40] |
| | | DJI Mavic Air 2 | 34 | 60 | Digital camera | Pavement pothole recognition based on UAV images. [40] |
| | | DJI Mavic Pro | 27 | – | Digital camera | UAV-based building damage detection and mapping system. [33] |
| | | DJI Mavic 2 | 31 | – | Digital & Thermal camera | Applying UAV to collect infrared and RGB images for automatic detection, classification, and localization of PV plants' defects. [36] |
| | | DJI Mavic 2 Pro | 31 | – | Digital camera | Crack detection of highway bridge piers utilizing UAV and lightweight networks. [41] |
| | | DJI Matrice 100 | 40 | – | Digital camera | UAV-assisted bridge 3D construction for UAV navigation and damage identification and analysis. [42] |
| | | DJI Matrice 200 | 38 | – | Digital camera | Applying UAV to detect corrosion and associated damages of bridge and sky rail. [43] |
| | | DJI Matrice 200 V2 | 38 | – | Thermal camera | Utilizing UAV and on-board infrared camera for classification of building heat loss damage. [38] |
| | | DJI Matrice 210 | – | – | Digital camera | UAV-aided bridge defect detection based on improved visibility images. [4] |
| | | – | – | 40 | Thermal camera | PV panel distress inspection from infrared images captured by UAV. [37] |
| | RTK | DJI Matrice 300 | 55 | 3 | Digital camera | Fine-grained crack detection of bridge through UAV-collected high-resolution images. [44] |
| | | – | – | 4–6 | Digital camera | 3D modeling for building exterior crack detection utilizing UAV. [45] |
| | | – | – | – | EL camera | An IoT-based cloud-edge computing system established for UAV-aided PV plant defects detection. [39] |
| | | DJI Phantom 3 Pro | 23 | – | Digital camera | Post-disaster building assessment based on multi-source data. [35] |
| | | DJI Phantom 4 | 28 | 75 | Digital camera | Pavement crack detection based on UAV images. [34] |
| | Hexacopter | DJI Phantom 4 Pro | 30 | 1.2 | Digital camera | Bridge inspection in terms of bolt-loosening detection from UAV images. [11] |
| | | DJI Phantom 4 RTK | 30 | 2 | Digital camera | Concrete building inspection of cracks in exterior walls from UAV images. [9] |
| | | DJI Matrice 600 Pro | 38 | 9/12/15/18/21/24 | Thermal camera | Bridge deck delamination detection and quantification utilizing UAV. [25] |
| | | Intel Falcon 8+ Customized | 26 | – | Digital camera | Bridge damage inspection through UAV. [28] |
| | | Customized | – | 2.5 | Digital camera | Assessment of seismic performance of deteriorated bridge structure by employing UAV-based damage detection. [46] |
| Customized | Quadrocopter | Customized | 30 | 2–4 | Digital camera | UAV image quality evaluating and enhancing in terms of bridge inspection. [29] |
| | | Customized | – | 4 | Digital camera | Bridge crack detection based on UAV. [47] |
| | | Customized | – | – | Digital camera | Quadrocopter control for altitude and crack recognition. [48] |
| | Hexacopter | Customized | – | – | Digital camera | UAV-aided real-time defect detection of transmission line dampers. [49] |
| | | Customized | – | 0.6–3.4 | Digital camera | Pavement crack detection and quantification from UAV images. [50] |
| | | Customized | 15 | – | Digital camera | Tunnel lining damage inspection. [51] |
| | Customized | – | – | – | Digital camera | Concrete building damage detection based on UAV images. [27] |

various rotary-wing UAVs in terms of commercial ones and customized ones. The specific parameters include type, classification, platform, maximum flight time, inspection distance, onboard sensors, and applications. As seen in [Table 2](#), most studies opted for commercial UAVs, with DJI being the most frequently used. It can be seen that studies employing customized UAVs lacked detailed parameters regarding maximum flight time, with only two papers providing these detailed information [[29,51](#)].

It is noteworthy that the endurance of UAVs does not significantly increase with the grow of rotor numbers. For instance, the Intel Falcon 8+ (8 rotors) has a maximum flight time of 26 min, the DJI Matrice 600 Pro (6 rotors) has a maximum endurance of 38 min, while the DJI Matrice 300 RTK (4 rotors) has a maximum endurance of 55 min. The endurance of UAV results from a combined effect of payload, battery capacity, and the quantity of rotors, for instance, DJI Matrice 100 has flight time of 28 min with one TB48D battery and no payload, when it is equipped with two TB48D batteries and no payload, the endurance only grows up to 40 min. The flight time does not double because higher battery capacity implies higher payload. Therefore, selecting appropriate sensing devices and UAV platform is crucial for maximizing detection efficiency based on specific detection tasks.

Since inspection distance is a key factor influencing the effectiveness of infrastructure surveillance, it is crucial to find the ideal detection distance to balance capturing sufficient details and maintaining efficiency. As summarized in [Table 2](#), for post-disaster building [[30,31](#)] and pavement inspections [[32–34](#)], data collection distances generally exceed 20 m. Notably, study [[35](#)] used three data sources to train the model for post-disaster building assessment: satellite, airborne, and UAV images, categorizing the data based on spatial resolution. Some studies conducted close-range inspection mainly involving bridges and buildings, with detection distances ranging from 1.2 to 6 m. In particular, study [[25](#)] carried out bridge deck delamination detection by collecting data from various time, distances, and angles to increase data diversity. [Table 2](#) also suggested that most of the studies used RGB images as data source, infrared cameras were typically used for inspecting specific structures or defects, such as Photovoltaic (PV) panels [[36,37](#)], heat loss defect [[38](#)], and delamination defect [[25](#)]. Additionally, one study utilized an Electroluminescence (EL) camera for PV plant inspection, EL images provide more reliable internal details of PV modules compared with thermal images. By injecting current into the PV modules, light emission will be caused and can be captured by image sensors [[39](#)].

3.1.2. On-board sensors

The selection and application of on-board sensors are crucial for UAV-based infrastructure inspection, determining the performance of data analysis. This section introduces the evolution, specifications, and applications of various on-board sensors for UAVs.

3.1.2.1. Evolution of UAV-mounted sensors. The development of sensors mounted on UAVs for infrastructure inspection has evolved significantly over the past decade. Initially, UAV-based inspections primarily relied on optical cameras for basic visual documentation. The earliest applications in civil infrastructure inspection utilized standard RGB cameras with limited resolution (typically 2–5MP) to capture visual evidence of surface damages. As UAV technology matured, higher resolution cameras (20–48MP) became standard, allowing for more detailed defect identification.

The evolution continued with the integration of specialized sensors to address the limitations of optical imaging. Thermal cameras were introduced around 2015–2017, enabling inspectors to detect subsurface anomalies and thermal variations indicative of structural issues. This represented a significant advancement as it allowed for the identification of delamination, moisture intrusion, and insulation issues not visible to the naked eyes.

The integration of LiDAR technology (approximately 2018–2020)

marked a new trend in UAV-based infrastructure inspection, transitioning from purely 2D visual analysis to comprehensive 3D structural assessment.

3.1.2.2. Optical images. Digital cameras are the most frequently used sensors in UAV-based infrastructure inspection. Optical images provide abundant visual information, including precise details of defect appearance, shape, and location, supporting the detection of various surface damages across multiple infrastructure types.

[Table 3](#) summarizes the types and specifications of airborne cameras applied in the retrieved papers. All cameras use Complementary Metal-Oxide-Semiconductor (CMOS) sensors due to their lower power consumption and high-speed reading capabilities, making them suitable for mobile devices like UAVs. The CMOS parameter indicates the physical dimensions of the image sensor, with larger sensors offering better light capture capabilities, reduced noise, and superior performance in low-light environments.

Camera resolutions range from 2MP to 48MP for various inspection tasks. Higher resolutions provide more feature information but require additional power. Field of view (FOV) affects the coverage area during inspection. Wide-angle FOVs (e.g., Zenmuse Z30 with 92°) are suitable for large-area scanning, while narrow FOVs (e.g., Zenmuse XT2 with 57.12°) offer more detail with less distortion. Cameras with moderate resolution and FOV (e.g., DJI Phantom 4 Pro) balance feature richness and coverage area, suitable for most surface inspection tasks.

3.1.2.3. Thermal images. Thermal cameras detect temperature distribution by capturing infrared radiation emitted by objects. This makes them suitable for detecting defects that manifest as temperature anomalies and uneven heat distribution, such as heat loss in buildings [[38](#)], bridge deck delamination [[25](#)], hotspot of PV plant [[36,37](#)], and sub-pavement voids of road surface [[52](#)].

[Table 4](#) summarizes thermal camera specifications used for inspection tasks. The resolution of thermal images (typically 640 × 512) is significantly lower than optical images. All thermal cameras in the reviewed papers operate in the long-wave infrared (LWIR) range (7.5–14 μm), suitable for detecting low-temperature features with cost-effectiveness and weather adaptability. Scene range modes (high-gain and low-gain) reflect sensitivity to temperature changes, with high-gain mode capturing subtle differences in lower temperature ranges and low-gain mode covering higher temperature ranges.

While thermal cameras generally have higher costs and lower resolution than digital cameras, they can operate independently of visible light, supporting all-day inspection and detection of internal damages of infrastructure, such as PV plant, bridge, based on temperature distribution.

3.1.2.4. LiDAR technology. LiDAR (Light Detection and Ranging) generates spatial point cloud data of the surrounding environment by emitting laser pulses and receiving light signals reflected from objects. The technology has evolved from simple 1D and 2D implementations to 3D systems.

In study [[46](#)], a 1D LiDAR, which measures distance in a single direction, was employed to sense the distance between UAV and the target, ensuring operational safety during flight. Study [[48](#)] used 2D LiDAR to obtain flight altitude for height control, enabling UAV navigation and improving flight stability.

3D LiDAR technology has significantly expanded UAV inspection capabilities. Modern UAV-mounted 3D LiDAR systems typically employ either mechanical scanning or solid-state technologies. Mechanical systems like the Zenmuse L1 (mentioned in [Table 3](#)) rotate multiple laser-detector pairs to achieve 360° horizontal coverage with up to 240,000 points per second and accuracy of ±5 cm. Solid-state systems sacrifice some field of view for reduced weight and power consumption, making them increasingly viable for UAV deployment. Zhao et al. [[53](#)]

Table 3

Specifications of the employed on-board digital cameras.

| UAV Platform | Camera | Sensor Type | Max Video Resolution & Frame Rate | Max Image Size | FOV | Weight (g) |
|------------------------|------------------|-----------------|-----------------------------------|----------------|--------------|------------|
| DJI Air 2S | Default camera | 1" CMOS | 4096 × 2160 30fps | 5472 × 3648 | 84 | – |
| DJI Inspire 1 | Zenmuse X5 | 4/3" CMOS | 4096 × 2160 23.98fps | 16.0MP | 72 | – |
| DJI Mavic Air 2 | Default camera | 1/2" CMOS | 3840 × 2160 60fps | 8000 × 6000 | 84 | – |
| DJI Mavic Pro | Default camera | 1/2.3" CMOS | 4096 × 2160 24fps | 4000 × 3000 | 78.8 | – |
| DJI Mavic 2 Enterprise | Default camera | 1/2" CMOS | 3840 × 2160 30fps | 8000 × 6000 | 84 | – |
| DJI Mavic 2 Pro | Default camera | 1" CMOS | 3840 × 2160 30fps | 5472 × 3648 | 77 | – |
| DJI Matrice 100 | Zenmuse Z3 | 1/2.3" CMOS | 4096 × 2160 25fps | 4000 × 3000 | 92 | 262 |
| DJI Matrice 200 | Zenmuse XT2 | 1/1.7" CMOS | 3840 × 2160 29.97fps | 12 MP | 57.12 | – |
| DJI Matrice 200 V2/210 | Zenmuse X5S | 4/3" CMOS | 4096 × 2160 29.97fps | 5280 × 3956 | 72 | 461 |
| DJI Matrice 300 RTK | Zenmuse H20 | 1/2.3" CMOS | 1920 × 1080 30fps | 4056 × 3040 | 66.6 | 678 |
| | Zenmuse H20T | 1/2.3" CMOS | 1920 × 1080 30fps | 4056 × 3040 | 82.9 | 828 |
| | Zenmuse L1 | 1" CMOS | 3840 × 2160 30fps | 5472 × 3648 | – | 930 |
| | Zenmuse P1 | Full frame CMOS | 3840 × 2160 60fps | 8192 × 5460 | 84/63.5/46.8 | 800 |
| DJI Phantom 3 Pro | Zenmuse Z30 | 1/2.8" COMS | – | 2.13 MP | 63.7 | 556 |
| | Default camera | 1/2.3" CMOS | 4096 × 2160 25fps | 4000 × 3000 | 94 | – |
| | Default camera | 1/2.3" CMOS | 4096 × 2160 25fps | 4000 × 3000 | 94 | – |
| | Default camera | 1" CMOS | 4096 × 2160 30fps | 5472 × 3648 | 84 | – |
| DJI Matrice 600 Pro | Default camera | 1" CMOS | 3840 × 2160 30fps | 5472 × 3648 | 84 | – |
| DJI Tello | Default camera | – | 1280 × 720 30fps | 2592 × 1936 | 82.6 | 80 |
| Intel Falcon 8+ | Sony Alpha 7R | Full frame CMOS | 1920 × 1080 60fps | 7360 × 4912 | – | 465 |
| Customized | Sony Alpha 9 | Full frame CMOS | 3840 × 2160 30fps | 6000 × 4000 | – | 588 |
| Customized | SIYI ZR10 | 1/2.7" CMOS | 2560 × 1440 30fps | – | 79.5 | 381 |
| Customized | Sony IMX219 | 1/4.0" CMOS | 1920 × 1080 47fps | 3280 × 2464 | 88 | – |
| Customized | Logitech LS20150 | 1/2.5" COMS | – | 2592 × 1944 | 160 | 4 |

Table 4

Specifications of the employed on-board thermal cameras.

| UAV Platform | Camera | Spectral Band (μm) | Scene Range (High Gain) | Scene Range (Low Gain) | FOV | Max Image Size | Weight (g) |
|---------------------------------|---------------------|--------------------|-------------------------|------------------------|-----|----------------|------------|
| DJI Mavic 2 Enterprise Advanced | M2EA thermal camera | 8–14 | –20 °C to 150 °C | –20 °C to 450 °C | – | 640 × 512 | – |
| DJI Matrice 200 V2 | DJI Zenmuse XT2 | 7.5–13.5 | –25 °C to 135 °C | –40 °C to 550 °C | – | 640 × 512 | – |
| DJI Matrice 210 | DJI Zenmuse XT | 7.5–13.5 | –25 °C to 135 °C | –40 °C to 550 °C | – | 640 × 512 | 270 |
| DJI Matrice 300 RTK | DJI Zenmuse H20T | 8–14 | –40 °C to 150 °C | –40 °C to 550 °C | – | 640 × 512 | – |
| DJI Matrice 600 Pro | FLIR Vue Pro R | 7.5–13.5 | – | – | 45 | 640 × 512 | 113 |

utilized Terrestrial Laser Scanning (TLS) and UAV imagery for 3D reconstruction of a high formwork project in Beijing, achieving a registration accuracy of 5 cm. Their method comprehensively captured geometric details and top structures, producing a complete, photo-realistic 3D model that significantly enhances construction management and digital documentation.

For bridge and tunnel inspection applications, study [54] integrated TLS with photogrammetry and deep learning for semi-automated inspection of concrete structures. TLS provided high-precision 3D geometry with 5 mm accuracy, while CNNs enabled crack detection, achieving effective defect localization in bridges and tunnels.

Despite the significant advantages of 3D LiDAR, current limitations include relatively high cost, substantial power consumption, and computational demands for processing large point cloud datasets.

3.1.2.5. Other sensors. It is notable that most of the articles implemented their studies by focusing on surface defects, such as crack, corrosion, and spalling. However, damage inside the structure can be as severe as surface defects without timely inspection and maintenance. Currently there are few studies utilizing on-board sensors other than camera and LiDAR to detect internal damage for comprehensive infrastructure inspections.

Other specialized sensors like EL cameras have been applied for UAV inspection. EL cameras detect light emitted by materials under electrical stimulation. In study [39], an EL camera was adopted for solar panel inspection due to its higher resolution and better sensitivity compared to thermal cameras, providing more precise defect assessment and localization.

Ultrasonic sensors have also been used in some studies. Ultrasonic sensors offer another non-destructive testing method for UAV-based infrastructure inspection, particularly valuable for measuring distances, detecting obstacles, and assessing material thickness or internal defects [55]. These sensors operate by emitting high-frequency sound waves and measuring the time taken for echoes to return after reflecting off surfaces or internal boundaries. Study [56] develops a vision-guided UAS for bridge underside inspection, in which an ultrasonic sensor, as a key component, was mounted on the UAV. It is used to measure the distance to the bridge underside in realtime, enabling automatic obstacle avoidance and ensuring the safe flight of UAVs in complex environments.

Ground Penetrating Radar (GPR) represents an emerging technology in UAV-based infrastructure inspection that enables subsurface assessment without contact or destructive testing [57]. UAV-mounted GPR systems emit electromagnetic waves that penetrate the surface and reflect upon encountering changes in material properties, allowing for the detection of internal voids, rebar placement, delamination, and moisture infiltration [58]. The integration of GPR with UAVs represents a promising direction for comprehensive infrastructure assessment, particularly for bridge decks, pavements, and concrete structures where internal defects significantly impact structural integrity.

However, the application of ultrasonic sensors and GPR in UAV-based inspection currently remains limited by several factors, including the requirement for close proximity or contact with the structure, and sensitivity to surface conditions.

3.1.2.6. Multi-modal data fusion. The integration of data from multiple

sensors, known as multi-modal data fusion, represents one of the most promising approaches for comprehensive infrastructure assessment. This approach leverages the complementary strengths of different sensing technologies to overcome their individual limitations and provide more complete structural information.

RGB-Thermal fusion has demonstrated particular efficacy in identifying complex defects. In [36], data fusion was employed by combining thermal and optical images to detect and classify defects in PV modules. The system uses IR images to identify thermal anomalies (e.g., hot spots) and RGB images to detect surface defects (e.g., dirt, vegetation), cross-validating the results to determine the root causes of hot spots. By integrating these data sources, the system achieves high accuracy in defect classification and provides detailed maintenance recommendations for PV plant operations. LiDAR-visual data fusion has shown remarkable potential for comprehensive structural assessment. Mirzaade et al. [54] implemented a multi-sensor fusion approach that integrated 3D LiDAR point clouds with high-resolution imagery for bridge inspection.

Despite the clear advantages of multi-modal sensing, significant challenges remain in terms of sensor synchronization, data registration, and the development of effective fusion algorithms. Additionally, the increased payload, power requirements, and computational demands of multiple sensors can significantly impact UAV flight performance and operational efficiency. When conducting infrastructure inspection, appropriate sensors should be selected based on specific application scenarios and tasks, considering the strengths and limitations of each sensing technology.

3.2. Inspected infrastructure and defect

This subsection presents types of UAV-surveilled civil infrastructures and corresponding distress concluded from the reviewed papers. UAV applications retrieved from reviewed papers can be concluded as defect

detection, defect mapping for quantification and localization, and post-disaster assessment.

Fig. 5 shows the 3-level categorization of UAV-assisted applications. Concluded from retrieved papers, infrastructure of construction, transportation, energy, water, and port are inspected. Specifically, 15 kinds of structures were inspected, which are buildings, bridge, pavement, railway, sky rail, embankment, tunnel, powerline, wind turbine, PV plant, water tower, dam, container crane, airport runway, and pipeline.

Statistics of annual publications of each type of civil structures were conducted for dynamic presentation of trend of UAV-based inspection as shown in **Fig. 6**. It is noticed that building inspection attracts the most attention with publication number of 45 in total. Another hotspot comes to bridge and pavement inspection with publication number of 22 and 17 respectively. Findings from **Fig. 6** suggest a rising research trend for structural assessment since 2021, which due to (1) development of UAVs makes it possible for large-scale inspection with higher flexibility and endurance ([59]); (2) Advances in deep learning technology have offered assurances in this field ([60]). **Fig. 7** also shows that surveillance of transportation, construction, and energy infrastructures constitutes 37.5 %, 32 %, and 25 % of the reviewed papers respectively, reflecting their dominance in modern infrastructure systems.

Table 5 concludes all types of civil structures and corresponding defects inspected in reviewed papers. As depicted in **Table 5**, infrastructures like bridge, pavement, building, PV plant, wind turbine, and powerline gained more attention by researchers with more defect types studied.

It is noticeable that crack is the commonest distress to almost every structure among all the detected distresses because the occurrence of crack is directly related to structure health and performance [45]. In particular, some studies implemented detailed classifications on specific defects for more refined detection, for instance, studies [26,32,61,62] divided crack into 5 types which are alligator crack, transverse crack, longitudinal crack, block crack, and oblique crack in terms of pavement

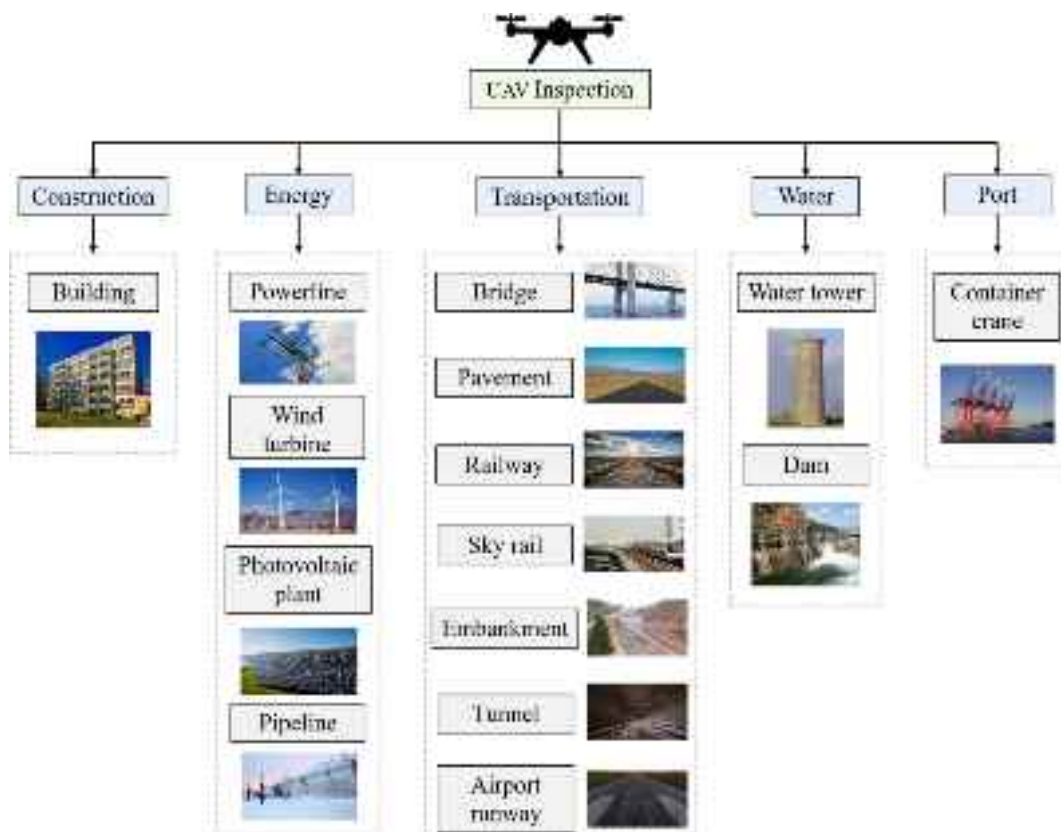


Fig. 5. Categorization of UAV applications in surveillance of civil infrastructure.

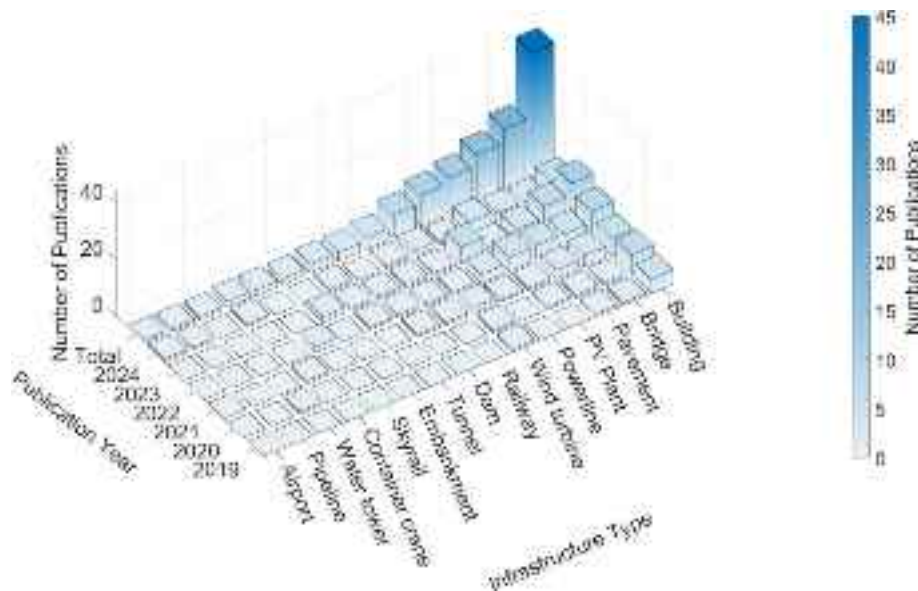


Fig. 6. Annual distribution of reviewed research across various infrastructure types.

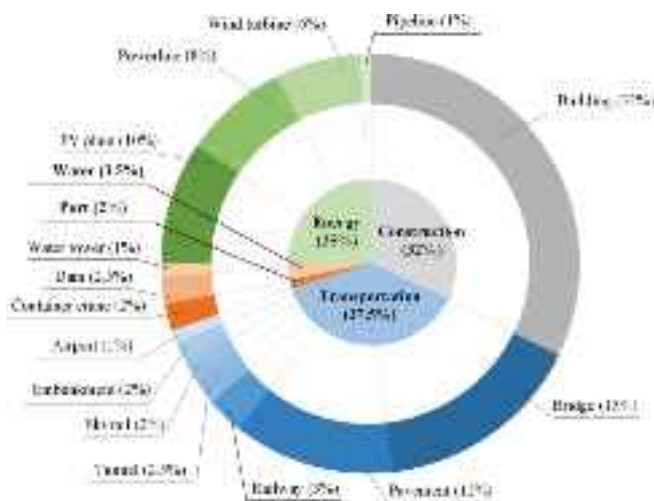


Fig. 7. Distribution of UAV applications in infrastructure inspection.

inspection.

Also, there are other defects that were divided into detailed levels, which are bridge corrosion (low level, medium level, and high level), pavement aging (early stage, middle stage, and late stage), PV plant hotspot (single and multi), and PV plant dirt (bird droppings, snail trails, snow, soil, dust, and cement). Based on different classifications, study [62] did a further investigation on the distribution of various distress with respect to distress sizes (small, medium, and large targets), which was defined according to the area taken by detection frame.

As for surveillance of powerline and railway, researchers focus more on smaller components because of their vulnerability and importance of insurance for system operation, detected parts include spike and clip of railway track, damper, bolt, nut, voltage balancing ring, bare conductor, and insulator of powerline.

It is noteworthy that tunnel inspection has received less attention, primarily due to the complexity of its environment. The lack of GPS signals inside tunnels makes UAV navigation and positioning more challenging, while also demanding higher obstacle avoidance capabilities [10]. Additionally, pipeline [63] and airport runway [64] have attracted increasing interest in terms of UAV-based inspection recently.

Except for specific defects detection, some researchers focused on

disaster response and resilience performance of post-disaster structures by implementing post disaster assessment. Table 6 summarizes studies related to post-disaster damage assessment among all the reviewed papers. Disasters of earthquake, hurricane, tornado, flood, wildfire, volcano, and tsunami are considered by researchers, among them earthquake draws the most attention. As shown in Table 6, post-disaster assessment was mostly conducted on buildings with damage level being briefly classified from undamaged to collapsed following inspection standards and evaluation manuals. Specifically, study [46] divided bridge damage level based on South Korea assessment criteria. As for post-disaster building assessment, present standard like EMS-98 [65], FEMA [66,67], and EF scale [68] are also utilized for division of damage levels. In addition, studies [69,70] carried out assessment with a different insight by recognizing various components of post-disaster buildings and surrounding environment through object detection or semantic segmentation, recognized components included flooded areas, debris, cars, roof, vegetation, wall, beam, window, balcony, column, slab, and background. Furthermore, in [1], the focus was placed on health assessment after completion of construction with damage level classified as undamaged, minor damage, moderate damage, and heavy damage.

3.3. Open-source datasets

Accurate and efficient damage detection is essential for subsequent infrastructure assessment. Key to this advancement is the availability of high-quality and multi-type datasets that are vital for robust model training. Field data collection can be restricted and hard-to-implement in specific areas, which hinders the subsequent model training, validating, and testing. Moreover, a lack of sufficient data volume cannot ensure the accuracy and generalization capability of deep learning models. All of the above-mentioned drawbacks indicate the importance of open-source datasets, which provide a solid foundation for the development of DL-based applications by offering data with abundant variety and volume. In this section, open-source datasets utilized in reviewed papers are concluded as shown in Table 7 with specifications of dataset name, number of images, scene, class, image type, resolution, and annotation.

As shown in Table 7, 32 currently available datasets dedicated to infrastructure defects detection are concluded in total with detailed descriptions of attributes in terms of number of images, scenes, classes, image types, resolutions, and annotations. From Table 7, the majority of

Table 5
UAV applications in identifying infrastructure defects.

| Type | Object | Defect |
|----------------|----------------|---|
| Transportation | Bridge | Crack, delamination, deformation, spalling/scaling, rebar/reinforcement exposure, water leakage, corrosion/stain, efflorescence/weathering, tilt, paint failure, split, bolt loosening, and corrosion. |
| | Pavement | Crack (alligator crack, transverse crack, longitudinal crack, block crack, and oblique crack), repair, pothole, aging (early stage, middle stage, and late stage), drainage issues, and polished aggregate. |
| | Railway | Spike free, clip free, rail split, ballast degradation, misalignment, vegetation, missing fastener, corrosive sound barrier, missing bolt, corrosive bolt, and loose bolt. |
| | Sky rail | Chromatic aberration and corrosion. |
| | Embankment | Crack. |
| | Tunnel | Crack, spalling, and leakage. |
| | Airport runway | Water pooling, vegetation encroachment, and runway smoothness. |
| | Building | Crack, spalling/peeling, rebar exposure, severely buckled rebar, heat loss, chromatic aberration, leakage, delamination, roof damage, efflorescence, and defacement. |
| | PV plant | Crack, vegetation, hotspot, open circuit, short circuit, DC box component, dirt (bird droppings, snail trails, snow, soil, dust, and cement), shadow, corrosion, light reflex, discoloration, delamination, and backsheet damage. |
| | Wind turbine | Crack, delamination, damaged, edge-damaged, rough, leading edge erosion, fatigue damage, broken VG (vortex generator), damaged lightning receptor, debris, oil spillage, misalignment, rigid coupling faults, and vibration problems. |
| Energy | Powerline | Damper inversion and deformation (slight and severe), insulation line (bare conductor), gasket missing (bolt), nut missing (bolt), corrosion (nut), skew and off (pressure balancing ring), pin missing (bolt), tightening pin failure (bolt), foreign object in place of tightening pin (bolt), flashover damage (insulator shell), broken (insulator shell), and missing (insulator). |
| | Pipeline | Insulation defects and product leaks. |
| | Water tower | Crack. |
| | Dam | Crack, concrete stone, water stain, spalling, voids and pits, precipitates, rebar exposure, and seepage. |
| | Container | Dirt, gland connection with rust, old repaint with new repaint, crack with repaint, rust, crack, fastener, exfoliation, nubby, and bar corrosion. |
| Port | Crane | Dirt, gland connection with rust, old repaint with new repaint, crack with repaint, rust, crack, fastener, exfoliation, nubby, and bar corrosion. |

the open-source datasets are constructed based on surface distress of pavement ([26,61,73,75,76,78,80,96,97]). Other datasets provide defects of bridges, buildings, powerlines, PV plants, wind turbines, and tunnels. According to content analysis of reviewed papers, no open-source defect datasets are found concerning container cranes, embankments, rails, sky rails, dams, and water towers.

It is worth noting that the dataset SDNET2021 [83] has made publicly available data from Impact Echo (IE), Ground Penetrating Radar (GPR), and Infrared Thermography (IRT). This dataset was collected from five in-service reinforced concrete bridge decks. The availability of IE, GPR, and IRT data enables researchers to move beyond surface-level investigations of bridges, providing a reliable foundation for further exploration of internal bridge damage and achieving comprehensive health monitoring of bridge structures. There are also another two datasets that are constructed on thermal images ([93,95]) regarding PV panel inspection.

Annotations of the listed datasets can be primarily categorized into two types: object-level and pixel-level. Object-level annotation involves enclosing the defect within a bounding box enabling precise localization

Table 6
Damage assessment of post-disaster civil infrastructure.

| Applications | Disaster | Damage Level | Assessment Criteria | Purpose |
|---------------------|---|--|---|--|
| Bridge | Earthquake | No damage, minor damage, moderate damage, major damage, and collapse damage | Bridge condition assessment criteria in South Korea | Seismic performance assessment of deteriorated bridge. |
| | Building | Intact and damaged | Not mentioned | Damaged building region detection. |
| | Earthquake | Component recognition (wall, beam, column, window frame, window pane, balcony, slab) | Not mentioned | Post-earthquake building component segmentation. |
| | Earthquake | Undamaged, slight, minor, major, and collapsed damage | EMS-98 standard [65] | Post-earthquake building damage detection. |
| | Hurricane | Undamaged, minor, moderate, severe, and destroyed damage | FEMA [66] and the HAZUS resistance model [71] | Post-disaster damage assessment. |
| | Hurricane and earthquake | Intact, partially, severe, and collapsed damage | EMS-98 [65] and FEMA [67] | Post-disaster damage assessment. |
| | Tornado | Minor, moderate, considerable, severe, devastating, incredible, and tarp | EF scale [68] | Post-disaster damage assessment. |
| | Post construction | Undamaged, minor, moderate, and heavy damage | Not mentioned | Post-construction building health inspection and assessment. |
| | Earthquake | Collapsed | Not mentioned | Post-disaster collapsed building detection. |
| | Earthquake | Undamaged, extensive, and collapsed damage | Not mentioned | Post-disaster damage assessment. |
| Hurricane and flood | Component recognition (flooded areas, debris, cars, vegetation, damaged roof, and undamaged roof) | Not mentioned | Post-disaster object detection. | |

of defects in the image. Except for localization, pixel-level annotations can identify the shape and contours of defects providing a more detailed depiction. It is noted that datasets with pixel-level annotations are considerably less voluminous than datasets built on object-level annotations, which is attributed to the intricate and labor-intensive nature of pixel-level annotation.

It can be found that data collection methods employed in most of the

Table 7
Identified Open-source Datasets.

| Dataset | Number of images | Scene | Class | Image type | Resolution | Annotation |
|---|--|---|---|---|-------------|--------------|
| CODEBRIM [72] | 1590 | Concrete bridges | Non-defective background, crack, spallation, exposed reinforcement bar, efflorescence, and corrosion. | Optical UAV images | – | Object-level |
| CrackForest [73] | 118 | Pavement | Crack. | Optical smartphone images | 480 × 320 | Pixel-level |
| DeepCrack [74] | 537 | Asphalt and concrete structures | Crack. | Optical images | 544 × 384 | Pixel-level |
| CrackTree200 [75] | 206 | Pavement | Crack. | Optical images | 800 × 600 | Pixel-level |
| CrackTree260 [76] | 260 | Pavement | Crack. | Optical images | 512 × 512 | Pixel-level |
| CRKWH100 [76] | 100 | Pavement | Crack. | Optical images | 512 × 512 | Pixel-level |
| CrackLS315 [76] | 315 | Pavement | Crack. | Optical images | 512 × 512 | Pixel-level |
| Stone331 [76] | 331 | Stone surface | Crack. | Optical images | 512 × 512 | Pixel-level |
| Tokaido Dataset [77] | 8648 | Concrete viaducts | Component: Slab, beam, column, nonstructural, rail, and sleeper. Damage: no damage, concrete damage, and exposed rebar. | Numerically generated synthetic images | 1920 × 1080 | Pixel-level |
| Crack500 [78] | 500 | Pavement | Crack. | Optical smartphone images | – | Pixel-level |
| COCO-Bridge [79] | 774 | Bridges | Components and defects: bearing (corrosion, connection, movement, alignment, bulging, splitting, tearing, and loss of bearing area), cover plate termination (fatigue-prone detail (cracking), section loss), out-of-plane stiffener (fatigue-prone detail (cracking), section loss), gusset plate connection (corrosion, cracking, connection, distortion, and damage). | Optical UAV images | 500 × 500 | Object-level |
| GAPs [80] | 1969 | Pavement | Crack, pothole, inlaid patch, applied patch, open joint, and bleeding. | Optical vehicle images | 1920 × 1080 | Object-level |
| Concrete Crack Images for Classification [81] | 40,000 | Concrete buildings | Crack and no crack. | Optical images | 227 × 227 | Object-level |
| SDNET2018 [82] | 56,000 | Concrete bridge decks, walls, and pavements | Crack and no crack. | Optical images | 256 × 256 | Object-level |
| SDNET2021 [83] | IE (483), GPR (663102), and IRT (4,580,680 pixels) | Concrete bridge decks | Sound, delamination above top bar mat, and delamination below top bar mat. | Image echo, Infrared thermography, Ground penetrating radar | – | – |
| Concrete Crack Conglomerate Dataset [84] | 10,995 (merged from open-source datasets) | Concrete structures | Crack. | Optical images | 512 × 512 | Pixel-level |
| QuakeCity [85] | 4688 | Buildings | Component: wall, column, beam, window, frame, and balcony Damage: spalling, crack, and rebar exposure. | Physics-driven UAV Visual images | 1920 × 1080 | Pixel-level |
| PEER Hub ImageNet [86] | 36,413 | Post-disaster structures | 1) Scene level: pixel level, object level, and structural level 2) Damage state: undamaged and damaged 3) Spalling condition: spalling and non-spalling 4) Material type: steel and others 5) Collapse mode: non-collapse, partial collapse, and global collapse 6) Component type: beam, column, wall, and others 7) Damage level: undamaged, minor, moderate, and heavy damage 8) Damage type: undamaged, flexural, shear, and combined damage. | Optical images | – | Object-level |
| Crack Segmentation Dataset [87] | 11,200 (merged from public datasets) | Pavement and concrete materials | Crack. | Optical images | 448 × 448 | Pixel-level |
| Tunnel919 [88] | 919 | Tunnel | Crack. | Optical images | 512 × 512 | Pixel-level |
| Crackseg9k [89] | 9255 (merged from open-source datasets) | Pavement, bridge, and other structures | Crack. | Optical images | 400 × 400 | Pixel-level |
| Insulator Defect Image Dataset [90] | 1596 | Transmission line insulators | Flashover damage insulator shell, broken insulator shell, good insulator shell, and insulator strings. | Optical images | – | Object-level |
| Wind Turbine Blade Surfaces Dataset [91] | 299 | Wind turbine blade | Damaged, edge-damaged, erosion, and rough. | Optical images | 8688 × 5792 | Object-level |
| PV-Net [92] | 45,754 | PV panel | Soiling (dust, snow, and bird drop) and defect (crack). | Optical images | 192 × 192 | Pixel-level |
| Photovoltaic Thermal Images Dataset [93] | 1009 | PV panel | One anomaly, not contiguous cells with anomalies, and contiguous cells with anomalies. | Thermal UAV images | 640 × 512 | Pixel-level |

(continued on next page)

Table 7 (continued)

| Dataset | Number of images | Scene | Class | Image type | Resolution | Annotation |
|---|------------------|------------------|---|-------------------------------------|--|--------------|
| DTU Drone Inspection Dataset [94] | 701 | Wind turbine | Leading edge erosion, vortex Generator panel (VG panel), VG panel with missing teeth, and lightning receptor. | Optical UAV images | – | Object-level |
| Photovoltaic System Thermal Images Dataset [95] | 277 | PV panel | Hot spots, snail trails, and sound cells. | Thermal UAV images | 336 × 256 | Pixel-level |
| RDD2022 [96] | 47,420 | Pavement | Longitudinal crack, transverse crack, alligator crack, and pothole. | Optical images with vehicle and UAV | 512 × 512, 600 × 600, 720 × 720, 3650 × 2044 | Object-level |
| Road Defect Dataset [61] | 2517 | Pavement | Longitudinal crack, transverse crack, alligator crack, and pothole. | Optical UAV images | – | Object-level |
| UAPD [26] | 3151 | Asphalt pavement | Longitudinal crack, transverse crack, alligator crack, oblique crack, pothole, and repair. | Optical UAV images | 512 × 512 | Object-level |
| Highway Crack Segmentation Benchmark Dataset [97] | 1157 | Pavement | Crack. | Optical UAV images | 512 × 512 | Pixel-level |
| PLD-UAV [98] | 11,202 | Powerline | Powerline (damaged/intact). | Optical UAV images | 540 × 360 | Pixel-level |

listed datasets include the use of smartphones, handheld cameras, vehicles, and UAVs. Remarkably, there are two datasets [77,85] generated based on realistic environments created by simulation softwares. Furthermore, datasets of Tokaido [77], COCO-Bridge [79], and QuakeCity [85] not only contain defect data, but also provide annotated information of infrastructure components from both object and pixel perspectives, facilitating subtle inspection tasks. Particularly, PEER Hub ImageNet dataset [86] provides eight sub-datasets, which are scene level, damage state, spalling condition, material type, collapse mode, component type, damage level, and damage type, designed to support diverse detection tasks.

3.4. Image data analysis

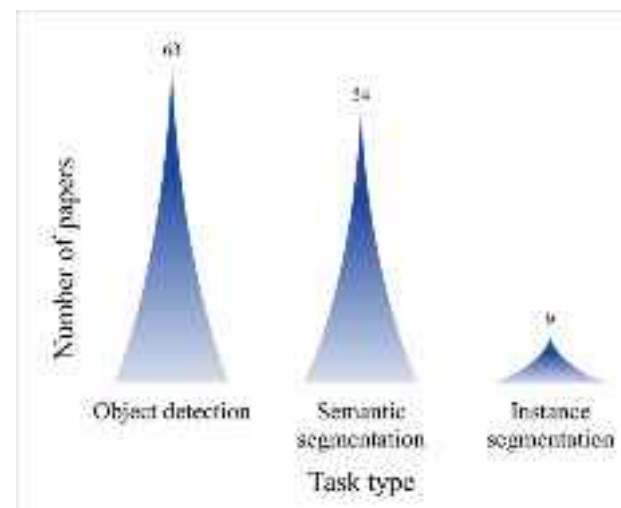
Selection and application of algorithms are crucial factors determining system performance and detection accuracy in terms of infrastructure inspection. To systematically explore the cutting-edge technologies in this field, this section provides a detailed description of various algorithms from two aspects: data preprocessing and deep learning models.

3.4.1. Data preprocessing

High-quality input data is a prerequisite for ensuring the effectiveness of deep learning models. Therefore, data preprocessing is of great importance as it enhances data quality and quantity while reducing noise and uncertainty during model training. To address the issue of insufficient data, many studies (e.g. [25,99,100]) employ data augmentation techniques, including rotation, scaling, flipping, color transformation, etc. Additionally, study [50] utilizes Generative Adversarial Networks (GANs) to generate defect images to expand the dataset. Regarding data quality issues, some research focused on image deblurring, study [101] employed Convolutional Neural Networks (CNNs) and GANs to enhance blurred defect images caused by UAV motion, while study [102] used the variance of the Laplace distribution to differentiate blurry from clear aerial images, and then applied the SRCNN model, designed for preprocessing image data, to address blurry images by converting poor-resolution pictures to super-resolution ones.

3.4.2. Deep learning models and applications

Through content analysis, damage detection methods can be primarily categorized into three approaches, as shown in Fig. 8: object detection, semantic segmentation, and instance segmentation. Notably, all three inspection methods employ CNNs or their variants as the backbone of models for feature extraction. The following subsections provide detailed descriptions of popular deep learning algorithms in

**Fig. 8.** Number of papers by task types.

infrastructure inspection field.

3.4.2.1. CNN and its variants. CNN plays a crucial role in feature extraction which are specifically designed for image data processing, spatial features extracting through convolutional layers, feature dimensions reducing via pooling layers, and classification performing through fully connected layers. CNN is effectively capable of capturing local and global information in images, enabling feature extraction and classification [103]. CNN forms the foundation of modern convolutional neural networks, which are CNN variants. During literature review, many studies applied CNN variants as feature extraction modules, which are called model backbones, for computer vision tasks. For instance, study [5] combines U-Net with VGG, ResNet, and Inception for defect detection. Table 8 summarizes CNN variants employed in reviewed papers. It is obvious that ResNet is the most commonly applied backbone which belongs to deep convolutional neural network (DCNN) architectures, with ResNet50 and ResNet101 being the most used, where the numbers indicate depth of the network.

Compared to traditional CNNs, CNN variants offer the following advantages: 1) the ability to capture more feature information, and 2) higher inspection accuracy. Although some DCNNs, such as VGG and ResNet, can achieve high-precision recognition, their computational cost is substantial, making them unsuitable for being deployed on

Table 8

Comparison of various architecture of CNN variants.

| Architecture | Key features | Versions |
|--------------|---|---|
| ResNet | Utilizes residual connections (skip connections) to address the vanishing gradient problem in deep networks, improving training depth. | ResNet-18, ResNet-34, ResNet-50, ResNet-101, ResNet-152 |
| VGG | Employs a simple and uniform convolutional block design (3×3 convolutions), with a deep architecture but high computational cost. | VGG11, VGG13, VGG16, VGG19 |
| Inception | Adopts multi-scale convolution kernels processed in parallel, integrating features at different scales. | Inception-v1 to v4 |
| Xception | Decomposes the convolutions in the Inception module into depthwise separable convolutions, improving model efficiency. | – |
| ConvNeXt | Modernizes ConvNet design with adjustments including deeper layers and more efficient architecture. | – |
| HRNet | Maintains high-resolution features by using parallel high-resolution and low-resolution branches, gradually fusing features. | – |
| EfficientNet | Uses compound scaling to simultaneously adjust network depth, width, and resolution, improving efficiency. | EfficientNet-B0 to B7 |
| ShuffleNet | Enhances efficiency with group convolutions and channel shuffle, suitable for mobile devices. | ShuffleNet-v1 to v2 |
| MobileNet | Uses depthwise separable convolution to reduce parameters and enable lightweight design for mobile and embedded devices. | MobileNet-v1 to v3 |
| DenseNet | Dense connections allow each layer to receive inputs from all preceding layers, which improve feature reuse and reduce parameters. | DenseNet-BC, DenseNet-201, DenseNet-264 |

resource-constrained devices. To address this issue, some studies (e.g., [104,105]) utilized lightweight neural networks like ShuffleNet, MobileNet, and EfficientNet to reduce computational and parameter requirements, improving model efficiency and real-time capability while maintaining reasonable accuracy.

Furthermore, some studies also employed Feature Pyramid Networks (FPN) to further process and fuse feature maps from the backbone to construct multi-scale feature maps [106]. Structure of FPN, including bottom-up pathway, top-down pathway, and lateral connections, addresses the limitations of CNNs and their variants in handling objects with different scales, enabling networks to better process objects with various sizes. FPN typically serves as the neck component in detection or segmentation tasks.

3.4.2.2. Transformer and its variants. While CNNs have dominated computer vision tasks in infrastructure inspection, Transformer architectures have recently emerged as powerful alternatives, bringing unique capabilities to defect detection and segmentation tasks. Transformers rely on attention mechanisms to capture global dependencies rather than the local feature extraction approach of CNNs.

Table 9 summarizes Transformers applied in reviewed papers. Based on statistics, Vision Transformer (ViT) and Swin Transformer are mostly used for infrastructure inspection mainly due to their capability of detecting small-scale defects [61].

Compared with CNNs, Transformers excel at capturing long-range dependencies across the entire image, which is particularly valuable for understanding structural relationships in infrastructure defects. Study [107] also suggested Transformer models have shown superior capacity in distinguishing between visually similar defect types.

Table 9

Comparison of various architectures of Transformer variants.

| Architecture | Advantages | Limitations |
|------------------------------|---|--|
| Vision Transformer (ViT) | Captures global dependencies across entire images enabling better performance for small defects; effective for large-scale patterns. | High computational cost; requires large datasets for training; limited performance on small defects. |
| Swin Transformer | Efficient modeling of multi-scale features; better performance for small defects; more parameter-efficient. | Requires significant computational resources compared to lightweight CNNs. |
| Mask2Former | Efficient modeling of multi-scale features; better performance for small objects; unified and parameter-efficient architecture for multiple segmentation tasks. | Requires significant computational resources; reliant on large-scale pretraining. |
| SegFormer | Efficient multi-scale feature representation; good balance between accuracy and computational cost. | Less effective for very fine-grained details compared to specialized CNN architectures. |
| DEtection TEansformer (DETR) | Suitable for damage detection with complex backgrounds without relying on anchor boxes or post-processing. | Converges slowly and is less sensitive to small objects with high computational cost. |

However, Transformer models also present significant challenges for UAV-based infrastructure inspection: computational demands, larger datasets requirement, and low inference speed. These issues can be critical factors for their real-time deployment on UAV systems. To address these limitations, hybrid approaches combining CNN and Transformer elements can be considered.

3.4.2.3. Object detection. Object detection is a computer vision task that can be briefly divided into single-stage and two-stage detection. As shown in **Fig. 9** it identifies and locates specific objects based on bounding boxes, with each box selecting an object in the image. Bounding box-based object detection algorithms can be used for various damage recognition, such as cracks, rust spots, spalling, rebar exposure, potholes, etc. **Table 10** summarizes object detection algorithms applied in retrieved papers.

As shown in **Table 10**, the most commonly used object detection algorithm is YOLO series. YOLO is a single-stage object detection algorithm that treats the detection task as a regression problem, directly predicting bounding boxes and categories from the input image. Its main advantage is fast detection speed, suitable for real-time applications.

Compared to single-stage algorithms, two-stage object detection algorithms can achieve higher detection accuracy by sacrificing computational speed. The two stages involve: 1) generating region proposals, 2) classification and bounding box regression for these regions. Two-stage algorithms such as R-CNN, Faster R-CNN are commonly applied for structural assessment.

In addition to previously mentioned algorithms, some researchers have attempted to use Transformers for object detection. In study [22], Semi-supervised Transformers were used to identify post-disaster buildings for damage level assessment. Notably, this study and some others ([49,108]) also employed Class Activation Mapping (CAM) to visualize model training progress by generating heat map to illustrate which area the model focuses more on when detecting a certain defect, improving model debugging and enhancing the interpretability of deep learning models.

Object detection approaches can identify and localize defects using bounding boxes, providing position and classification information. Based on reviewed papers, object detection models are particularly valuable for multi-class defect identification [49] and defect enumeration [28]. However, object detection has limitations for infrastructure inspection, including imprecise defect boundary delineation and



Fig. 9. Example of object detection ([2]).

Table 10
Algorithms for object detection.

| Category | Name | Versions | Key features |
|--------------|--------------|---------------------------------|--|
| Single-stage | SSD | SSD300, SSD512 | Multi-scale feature maps and direct bounding box regression. |
| | YOLO | YOLO-v1 to v8 | Transforms object detection into a regression problem, directly predicts bounding boxes and class probabilities. |
| | EfficientDet | EfficientDet-D0 to D8 | Combines EfficientNet's compound scaling strategy, introduces Bi-directional Feature Pyramid Network (BiFPN). |
| Two-stage | R-CNN | R-CNN, Fast R-CNN, Faster R-CNN | Region proposals + Convolutional Neural Networks, first generates candidate regions, then performs classification and bounding box regression. |

difficulty in measuring defect dimensions accurately.

3.4.2.4. Semantic segmentation. Semantic segmentation aims to classify each pixel in an image to divide it into different semantic categories. Unlike object detection methods, semantic segmentation not only locates objects but also precisely delineates their shapes and boundaries, as shown in Fig. 10. Semantic segmentation can be used for various defects ([44,46,109,110]) or structural component ([69,104,105,111]) identification and assessment with crack being the mostly detected defect. Table 11 shows algorithms commonly used for supporting data segmentation in defect recognition tasks.

As evident from the table, most studies choose U-Net as segmenting algorithm. U-Net is the most classic semantic segmentation network initially proposed by Ronneberger et al. [112]. It adopts a symmetrical U-shaped structure, including an encoder and a decoder.

The encoder gradually extracts high-level features of the image, while the decoder progressively restores spatial resolution, generating accurate pixel-level classification results. Study [113] combined CNN with U-Net for a two-step bridge crack segmentation and achieved a precision of 97.4 %.

As a lightweight model, CrackNet [114] is suitable for UAV real-time

inspection because it is parameter-friendly. SAM [115] is a Transformer-based segmentation model that supports zero-shot segmentation. While its encoder, built on Vision Transformer (ViT), has high computational demands, the decoder is designed to be lightweight and suitable for edge devices. However, its overall computational efficiency still falls short compared to CrackNet.

Even though semantic segmentation enables precise measurement of defect dimensions and shapes, The main limitations still exist. Limitations of semantic segmentation include inability to distinguish between adjacent instances of the same defect type and higher computational requirements compared to object detection.

3.4.2.5. Instance segmentation. Fig. 11 shows an example of instance segmentation. Instance segmentation is an extension of semantic segmentation, requiring not only the classification of each pixel in the image but also the differentiation of different instances within the same class. Instance segmentation has important applications in infrastructure inspection as it can accurately detect and distinguish multiple defect instances, which is key information for subsequent data quantification and management. Table 12 illustrates algorithms for instance segmentation employed in reviewed papers.

In study [105], an improved Mask R-CNN model was used for post-disaster building assessment, using instance segmentation with different colors to grade the degree of building damage. Study [116] employed Mask R-CNN to detect cracks on building external walls and mapped them to a 3D reconstructed model for data management at each defect level, with cracks segmented in different colors reflecting detailed features.

The development of instance segmentation considers the limitations of object detection and semantic segmentation. It can provide both precise defect boundaries and instance differentiation, which is most valuable for complex environments with overlapping defect [105] and severity classification of individual defects [117]. Due to the combination of object detection and semantic segmentation, instance segmentation requires higher computational demands and presents slower inference speeds.

3.4.2.6. Performance comparison of deep learning models. For better reference of choices for DL models, we summarize the practical

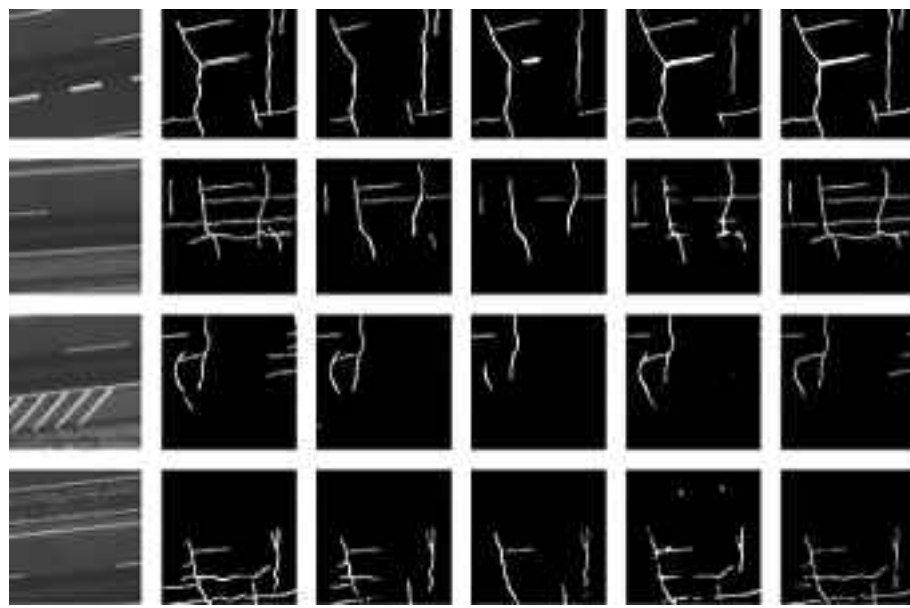


Fig. 10. Example Of semantic segmentation ([97]).

Table 11
Algorithms for semantic segmentation.

| Name | Versions | Key features |
|------------------------------|---|--|
| FCN | – | Fully convolutional network, end-to-end training and prediction, supports input images of arbitrary sizes. |
| U-Net | U-Net, U-Net++ | Encoder-decoder structure, skip connections, suitable for small datasets. |
| U ² -Net | – | Dual U-structure, captures more detailed information, suitable for object segmentation in complex backgrounds. |
| SegNet | – | Encoder-decoder structure, uses max-pooling indices for upsampling, reduces computation. |
| DeepLab | DeepLabv1, DeepLabv2, DeepLabv3, DeepLabv3+ | Introduces atrous convolution, extracts multi-scale features, combines fully connected conditional random fields (CRF) to improve segmentation accuracy. |
| CrackNet | – | Utilizes CNNs to achieve pixel-level segmentation of cracks. |
| DeepCrack | – | Using multi-scale feature fusion mechanism to capture crack details and global context by integrating hierarchical features. |
| PSPNet | – | Employs a pyramid pooling module to capture multi-scale contextual information. |
| Segment Anything Model (SAM) | – | Zero-shot segmentation via prompts (e.g., points, boxes) and applicable for diverse image segmentation tasks without task-specific training data. |

performance of different models in terms of key metrics based on various inspection tasks (object detection, semantic segmentation, and instance segmentation). Table 13 presents a comparison of various deep learning models applied to infrastructure defect detection tasks across different structures and defect types. This comparative analysis reveals several important patterns in model selection for UAV-based inspection applications.

A notable observation from the performance metrics is the variability



Fig. 11. Example Of instance segmentation ([116]).

Table 12
Algorithms for instance segmentation.

| Name | Key features |
|--------------------|---|
| Mask R-CNN | Adds a branch for instance segmentation on top of Faster R-CNN, generates pixel-level segmentation masks. |
| Mask Scoring R-CNN | Adds a scoring branch on top of Mask R-CNN to improve the accuracy and quality of generated masks. |

in model accuracy across infrastructure types and defect categories. For instance, U-Net achieved an mIoU of 0.926 for PV plant defect segmentation in study [122], far surpassing its 0.792 mIoU for dam crack segmentation in study [123], highlighting the influence of inspected structures on model performance.

The comparison also reveals a trade-off between computational efficiency and detection accuracy. When inspecting the same infrastructure, faster inference ability means lower detection accuracy. In study [119], single-stage detectors like YOLOv5s and YOLOv8s offer faster inference times than two-stage detectors like Faster RCNN, making them ideal for real-time UAV inspections with limited onboard processing by sacrificing a certain level of detection accuracy.

It is also noticeable that bounding box-based inspection strategies are

Table 13
Model comparison.

| Reference | Task | Model | Performance metrics | Frames Per Second (FPS) | Infrastructure type | Defect type |
|-----------|-----------------------|----------------------------------|--|-------------------------|---------------------|---|
| [2] | Object detection | YOLOv6s | mAP@50 = 64.8 % | 290 | Bridge | Spalling, exposed rebar, and efflorescence. |
| | | YOLOv6s + GFPN | mAP@50 = 67.6 % | 270 | | |
| [118] | Instance segmentation | Mask RCNN | mAP@50 = 93.6 % | 1.23 | Bridge | Crack, exposed bar, spalling, efflorescence, and viod. |
| [117] | Instance segmentation | Mask Scoring RCNN | mAP@50 = 94.6 % (Detection result), mAP@50 = 86.9 % (Segmentation result) | – | Powerline | Good insulator and defective insulator. |
| [119] | Object detection | YOLOv5s | mAP@50 = 74.0 % | 127.42 | Pavement | Crack. |
| | | YOLOv8s | mAP@50 = 77.1 % | 125.74 | | |
| | | Faster RCNN | mAP@50 = 79.3 % | 12.8 | | |
| [120] | Object detection | Faster RCNN | mAP@50 = 64.0 % | 10.14 | Building | Shear, flexural, combined damage, and undamaged. |
| [121] | Object detection | FasterRCNN+ Few-shot Fine-tuning | mAP@50 = 38.0 % | 223.4 | Railroad | Missing bolt, corrosive bolt, Loose bolt, and corrosive sound barrier column. |
| [122] | Semantic segmentation | UNet | mIoU = 0.926 | 1.54 | PV plant | Bird droppings, cement, crack, soil, and no damage. |
| [123] | Semantic segmentation | UNet+VGG backbone | mIoU = 0.981 | 0.58 | | |
| | | UNet | mIoU = 0.792 | 7.3 | Dam | Crack. |
| | | FCN | mIoU = 0.565 | 0.1 | | |
| | | DeepLabV3+ + MobileNetV2 | mIoU = 0.623 | 9.9 | | |

more computational-friendly than segmentation methods with suppressed detection accuracy. In study [118], an instance segmentation approach for bridge defect analysis achieved an exceptional detection accuracy (mAP@50 = 93.6 %) for the object detection component, significantly outperforming the object detection approach in study [2]. However, this superior performance came at the cost of inference speed, which was nearly 200 times slower than object detection models. Such extreme difference highlights the critical importance of clarifying inspection priorities.

According to study [117], the difference of detection result (94.6 % mAP@50) and segmentation result (86.9 % mAP@50) for the same defect and structure suggest the possibility of the superiority of bounding box-based methods. Although replacing the detector with a few-shot strategy can effectively address the issue of data scarcity, a comparison of experimental results from studies [120,121] shows that, due to insufficient training data, adopting few-shot fine-tuned detector shows the possibility of reduced detection accuracy of models.

In summary, model selections depend on infrastructure, defects, and inspection priorities, no single model excels universally. Lightweight models like YOLO or MobileNet-based architectures represent practical choices despite their accuracy compensation. Conversely, heavier models like Faster R-CNN, DeepLabV3+, or Mask R-CNN offer superior detection capabilities that justify their higher computational demands, which is excel for post-flight analysis.

3.4.2.7. Route planning for efficient inspection. While deep learning algorithms are critical to defect detection, efficient UAV route planning is essential for comprehensive data collection. Route planning directly impacts inspection efficiency, image quality, and UAV endurance.

Hu et al. [124] introduced a UAV path planning method for post-disaster response, utilizing building damage information to optimize task allocation and path computation. Among the evaluated algorithms—Genetic Algorithm, Ant Colony Optimization, Particle Swarm Optimization, and BITmask Evolutionary Optimization (BITEOPT)—BITEOPT consistently delivers the best performance, efficiently determining optimal paths. By incorporating deep learning for damage detection, this method significantly improves UAV task planning efficiency, enhancing the effectiveness of disaster response operations.

Rahman et al. [125] proposed a UAV path planning strategy for insulator inspection in low-voltage distribution systems, using a 270° circular path and a straight path with a 180° rotation. Results suggested that straight path is more efficient (F1-score of 0.81) and safer. This

semi-autonomous method highlights the role of path plannings in improving inspection accuracy and operational safety.

The integration of intelligent route planning with deep learning-based detection systems represents an important frontier in UAV-based infrastructure inspection, maximizing both inspection coverage and the quality of data available for defect analysis.

4. Discussion

Despite significant advances in this field, several challenges and limitations still remain that affect UAV-oriented practical implementation and widespread adoption. To facilitate the development of UAV-based infrastructure inspection, this section discusses current challenges from three key perspectives: limitations of UAV platforms, inadequacies in public datasets, and constraints in DL algorithm applications. Following this discussion, future research directions are proposed to address these challenges and further enhance inspection capabilities. These directions focus on UAV platform optimization, dataset development strategies, and DL algorithm improvements that aim to create more robust, efficient, and practical inspection solutions for various infrastructure types under diverse environmental conditions.

4.1. Current gaps and challenges

Despite the significant potential of combining UAV with deep learning for damage detection, challenges and gaps still remain. This section systematically analyzes the difficulties encountered when applying UAVs for structural inspection from three perspectives: UAV platforms, publicly available datasets, and deep learning algorithms. Detailed analysis is illustrated in the following subsections.

4.1.1. Limitations of UAV platforms

Although UAVs possess advantages such as high flexibility, excellent maneuverability, and enhanced efficiency with respect to infrastructure inspection, there are still several drawbacks which can be improved for better performance. One major limitation is the endurance of UAVs. As evidenced in reviewed papers, the average recorded flight time for UAVs is around 30 min. This limited endurance poses significant challenges for continuous and efficient data capturing of large-scale structures. For instance, in study [61], the authors needed to use multiple batteries to complete the inspection task of PV panels, which lowered the inspection efficiency due to downtime.

Furthermore, environments with absent or weak GPS signals pose significant challenges to UAVs. These challenges include inaccurate positioning, reduced flight stability, and compromised data precision, all of which increase operational risks [29,46]. Tunnels, as one of the typical structures that often experience GPS signal loss, are not extensively studied in reviewed papers. Only three articles utilized UAV for tunnel inspection [51,54,126], underscoring the restrictive impact of GPS signal absence on UAV applications. It was also found that 80 % of the reviewed studies employed commercial UAVs, especially DJI UAVs. However, the software of commercial UAVs are usually closed-source, preventing users from performing coding, which limits the possibility of secondary development such as UAV path planning and UAV swarm.

4.1.2. Limitations of open-source datasets

Currently used open-source datasets for DL-based infrastructure defect inspection are relatively limited and predominantly focus on a single type of defect, primarily related to road surface cracks. Moreover, these datasets often lack complexity in backgrounds, the majority of collected data are under clear weather conditions, with less emphasis on adverse conditions such as overcast, rainy days, or shadows. However, supplement of data captured from poor weather conditions is crucial for enhancing model performance, for instance, contrast between background and defects decreases when structure surface becomes wet, which would complicate detection process and increase generalization ability of DL models.

It is also noted that public datasets suitable for segmentation tasks are scarce. This scarcity is attributable to the intricate and labor-intensive nature of pixel-level data annotation. However, data volume, data diversity, and data complexity are decisive factors in improving the accuracy and generalization capabilities of deep learning models.

Another limitation is the imbalance in terms of the amount of different classes provided by public datasets, for instance, dataset [72] has 2507 instances of cracks but only 833 instances of efflorescence. This imbalance can lead to models having higher detection capabilities for certain types of distress while performing poorly on others, thereby reducing the overall accuracy. Additionally, there is a lack of an unified standard for defect annotation in current open-source datasets. With the inconsistencies in data annotation, model outputs can become less predictable. As mentioned in [79], corrosion and stain are classified as the same kind of defect in some studies. Defect of delamination in study [127] is annotated as “damaged” in [128]. Inconsistencies in data annotation can pose significant challenges when attempting to train models using multiple open-source datasets. Thus, it is necessary to re-annotate these datasets to ensure data uniformity, which is crucial for the effective training and better performance of deep learning models.

Furthermore, dataset annotation still relies on manual labor to a large extent, which is cost-intensive and time-consuming, especially for pixel-level annotations that require elaborate focus on every pixel. Therefore, there is an urgent need for a more lightweight and efficient annotation method to support the large-scale data demand required by DL training.

4.1.3. Limitations of algorithm applications

Despite the significant advancements in DL algorithms, their application in automated infrastructure inspection still faces several challenges. Overfitting still remains a primary concern, models showing overfitting usually perform well on training data but struggle with new data, which significantly reduces their generalization capability. This phenomenon is particularly pronounced in infrastructure inspection tasks, where training datasets often fail to encompass all possible environmental conditions and damage types.

Current DL models also exhibit limitations in transferability. The same type of defect (e.g., cracks) may occur across various infrastructures, models trained on a specific infrastructure (such as bridges) often struggles to be directly applied to the detection of similar defects appeared on other structures (like building exteriors). This is due

to the significant differences in surface features and environmental backgrounds of various infrastructures, where models find challenging to adapt to.

Besides, many studies rely on data collected from fixed detection distances for model training. However, in practical applications, detection distances may vary due to selection of sensing devices and inspecting targets. This inconsistency in data collection, particularly in terms of feature richness and damage scale, further impacts model performance. Moreover, current detection algorithms are still at the stage of model training and validation based on offline data. While this approach performs well in static environments, it lacks real-time performance adaptability in dynamic settings. Additionally, deep learning models typically involve numerous parameters and complex computational processes, making it difficult for high-complexity models to run in real-time on UAV platforms usually with limited computational capabilities.

4.2. Future research trends

Infrastructure inspection is crucial in civil engineering, as it significantly enhances the longevity of structures and ensures public safety. Although current UAV and DL-based inspection technologies have achieved notable progress, several limitations and challenges still remain. The existing public datasets still fall short in terms of data quality and diversity. Additionally, current algorithms need further improvement to manage complex scenarios and enhance detection accuracy. Furthermore, UAV platforms face certain limitations in terms of endurance and environmental adaptability. Consequently, this section proposes future research directions for these difficulties and aims to further improve the efficiency and accuracy for defect detection.

4.2.1. UAV platform optimization

The primary challenge in deploying UAVs for infrastructure inspection is their limited endurance. According to the reviewed literature, the average maximum flight time for commercial UAVs is approximately 30 min, which is insufficient for comprehensive surveillance of extensive infrastructure systems. To address this critical limitation, future research can focus on several promising approaches.

First, UAV swarm deployment offers a compelling solution. Systems comprising multiple collaborating UAVs can significantly enhance operational efficiency and coverage by distributing inspection tasks across multiple platforms, thereby decrease individual battery constraints. Study [129] proposed a distributed communication architecture for remote management of UAV swarms monitoring solar power plants, which automatically generates flight paths based on plant layout and optimizes mission execution with minimal human intervention. Future research could focus on developing advanced swarm coordination algorithms that ensure continuous operation while minimizing downtime for battery replacement or recharging.

Second, optimized route planning algorithms present significant potential for extending operational duration. Path planning that accounts for infrastructure geometry, inspection demands, and energy consumption can substantially improve inspection efficiency. Mirzazade et al. [130] optimized UAV flight paths to ensure efficient and accurate data collection during bridge inspections. Future research is suggested to explore the integration of reinforcement learning and other adaptive algorithms to develop path planning strategies that dynamically respond to changing environmental conditions.

Advancements in UAV control systems design offer another promising solution for endurance enhancement. Inspired by study [131], customized UAV hardware improvements could incorporate hybrid power systems combining solar cells, lithium-polymer batteries, and supercapacitors with lightweight voltage regulators to extend flight time while reducing charging duration. Alternatively, control strategy optimization, such as algorithms that minimize power consumption during different flight phases (hovering, cruising, etc.), could also extend

operational duration without hardware modifications.

Another significant challenge for UAV-based inspection systems is navigation in GPS-denied environments. Many critical infrastructure components, such as bridge undersides and tunnels, lack reliable GPS signals, necessitating alternative navigation approaches. Wang et al. [132] proposed a ground-aerial collaborative system where ground vehicles serve as a guidance platform with infrared markers mounted on top, while UAVs use 45° downward-tilted Intel RealSense D455 cameras for positioning and upward-facing 4 K cameras for defect inspection of bridge undersurfaces. Jiang et al. [56] combined ultrasonic sensors with stereo vision-inertial fusion methods to provide positioning and obstacle avoidance capabilities in GPS-denied environments beneath bridges. To solve this problem, future research could focus on enhancing the robustness and reliability of visual and autonomous navigation systems in challenging environments through the integration of various sensors including visual, inertial, LiDAR, and ultrasonic systems [10].

4.2.2. Public dataset development and enhancement

During UAV flights, various internal factors (e.g., exposure times, sensor performance) and external factors (e.g., wind, rain) can affect the quality of collected data. As the key factor for determining accuracy of DL models, low-quality data diminishes model capability of identifying distress and data recollection can significantly reduce inspection efficiency. Also the quality of data provided by open-source datasets varies, which makes it hard to integrate various datasets for training data enlargement. To address this, inspired by the study [29], future research can focus on data quality assessing and enhancing before model training, thereby reducing the need for repetitive data collection.

It is also noted that the same type of defect is commonly labeled differently across various studies. In study [127], dust and soil are classified as dirt, while in study [133], the defect soil is identified as permanent soiling, leading to inconsistency of annotation in public datasets. Such discrepancies pose significant challenges to the performance of deep learning models. To address this issue, establishment of a standardized defect annotation criteria is suggested. This standard should include detailed definitions of defect types for various infrastructure, annotation guidelines, and examples to ensure label consistency across different studies and public datasets. Such standard can improve data compatibility and comparability, thereby enhancing training effects and generalization capabilities.

Besides, current public datasets exhibit a notable limitation in their predominant focus on crack detection, resulting in imbalanced class distributions that diminish model performance for other defect types. Future research can address this limitation through several approaches.

Synthetic defect data generation using simulation software that replicates UAV perspectives can reduce data collection costs and difficulties. Studies [69,134,135] utilized simulation software to generate post-disaster damage data, enabling damage assessment across different infrastructure components. For scenarios requiring substantial data volumes or involving high annotation costs, active learning methods can be considered. Study [63] demonstrated how active learning can optimize annotation efficiency by selectively identifying the most valuable samples for subsequent labeling during training.

Domain adaptive learning offers promising solutions for addressing data scarcity or imbalanced data distributions [107]. Studies by Li et al. [136] and Gwon et al. [137] utilized Generative Adversarial Networks (GANs) to generate target domain data or transform source domain data to target domain styles, effectively addressing data imbalance issues. Transfer learning through pre-trained backbone networks provides another valuable approach. Khankeshizadeh et al. [5] enhanced U-net model feature extraction capabilities through transfer learning, significantly improving post-earthquake building damage detection accuracy and generalizability. Another trend for addressing data scarcity is few-shot learning methodologies by enabling effective learning from extremely limited samples. Hong et al. [121] introduced a few-shot detector specifically designed to address data limitations in post-

disaster building damage assessment, while Li et al. [138] employed a single-shot multibox detector combined with pre-training and data augmentation strategies to overcome data insufficiency in similar applications.

Automatic data annotation represents another promising direction for addressing the shortage of labeled data in public datasets. Studies [139,140] demonstrated how combining computer vision techniques with pre-trained models (such as object detection or semantic segmentation networks) can provide preliminary annotations for unlabeled data, requiring only minimal expert correction and thus substantially reducing manual annotation workload.

The above-mentioned methods, synthetic data generation, active learning, domain adaptive learning, transfer learning, few-shot learning, and automatic annotation, not only effectively address data scarcity and distribution imbalance but also significantly reduce time requirements, thereby enhancing both the efficiency and performance of infrastructure defect detection systems.

4.2.3. Deep learning algorithm enhancement

To address various challenges encountered in deep learning-assisted infrastructure inspection applications and enhance their performance in practical scenarios, future research could focus on improving model accuracy, enhancing generalization ability, and optimizing real-time processing capabilities.

Model accuracy improvement represents a critical direction for future research. Current deep learning models often struggle with detecting small or subtle defects under varying environmental conditions. The introduction of Transformer architectures offers new possibilities for further improving model precision. With their self-attention mechanisms, Transformers can better capture dependencies between global and local features within images, which is valuable for detecting subtle defects. Recent studies indicate that hybrid models combining Transformers with convolutional layers (such as Vision Transformers or Swin Transformers) demonstrate excellent performance in infrastructure defect detection tasks [51]. Additionally, attention mechanisms that focus model computation on regions of interest within images show considerable promise. Li et al. [141] incorporated Convolutional Block Attention Module (CBAM) and Simple Attention Module (SimAM) into YOLOv7, achieving a 5.6 % improvement in defect detection accuracy compared to original architectures. Future research could further explore optimizing Transformer computational efficiency, such as lightweight Transformer SegFormer [142] and MobileViT [143], and designing hierarchical attention mechanisms for the multi-scale and multi-modal features of defects.

Multi-source data fusion brings new ideas for enhancing inspection capabilities. Integration of data from different sources, such as visual, thermal, LiDAR, ultrasonic, and GPR, can provide a more comprehensive expression of infrastructure conditions. For instance, Kuo et al. [36] combined infrared imaging for PV panel hotspot detection with RGB imaging for surface contamination or vegetation coverage detection, enabling cross validation to determine specific causes of thermal anomalies. Similarly, Zhao et al. [53] demonstrated that integrating 3D point cloud with visual imagery enabled more accurate geometric quantification of structural defects. Future research is suggested to explore advanced multi-source data fusion approaches to further enhance detection capabilities.

To address variations in detection conditions caused by environmental factors during field inspections, multi-scale feature extraction approaches requires further investigation. Pyramid network architectures that process features at multiple resolutions have shown promising results in handling scale variations in defect detection tasks. Liu et al. [74] proposed a deep feature pyramid network-based crack segmentation method that effectively handles cracks of various scales presented in bridges, roads, and other infrastructure through multi-scale feature fusion. Future research could focus on developing adaptive multi-scale architectures that dynamically adjust their receptive fields based on

detection conditions, ensuring robust performance across diverse inspection scenarios.

Finally, enhancing real-time performance remains critical for practical deployment of deep learning models on UAV platforms with limited computational resources. Light-weight algorithms specifically designed for edge deployment, such as MobileNet [144] and EfficientNet [145], draw significant attention. Study [146] proposed a lightweight CNN model specifically designed for damage detection on resource-constrained embedded systems like UAVs. Their experimental results indicated that the model's average precision was only 1.2 % lower than the YOLOv5 model while achieving higher frames-per-second processing rates than other benchmark models. Edge computing integration can further improve real-time responsiveness by distributing computational tasks between UAV platforms and ground stations, reducing data transmission latency and enabling more timely detection of critical defects. The above-mentioned strategy can also increase flight time of UAVs in terms of practical deployment of deep learning models.

By focusing on these research directions, the field can make significant progress toward developing more accurate, robust, efficient, and lightweight deep learning solutions for UAV-based infrastructure inspection, ultimately enhancing the safety and reliability of civil infrastructure systems.

5. Conclusions

This review examined the integration of UAV platforms and deep learning technologies for infrastructure inspection and defect detection, highlighting both the advances and challenges in this rapidly evolving field. As civil infrastructure continues to age, the need for efficient, accurate, and cost-effective inspection methods has become increasingly critical. The combination of UAVs and deep learning has emerged as a promising alternative to traditional manual inspection approaches, offering enhanced safety, efficiency, and detection capabilities.

This review also revealed that UAV-based inspection systems have been successfully deployed across diverse infrastructure types, from bridges and buildings to roads and energy facilities. The flexibility and maneuverability of UAVs, equipped with various sensors, enable comprehensive data acquisition even in hard-to-reach areas. Meanwhile, deep learning algorithms have demonstrated exceptional capabilities in automatically detecting multiple defect types with increasing accuracy.

Nevertheless, significant challenges persist across three key perspectives. First, UAV platforms face limitations in flight endurance and operation in GPS-denied environments. Second, public datasets exhibit insufficient diversity, imbalanced class distributions, inconsistent annotation standards, and inadequate data with complex backgrounds. Third, current deep learning algorithms struggle with detection accuracy and difficulties in real-time deployment on resource-constrained UAV platforms.

To address these challenges, some promising research directions were proposed. For UAV platforms, future development could focus on enhancing endurance through UAV swarm deployment, optimized route planning, and advanced control system design, while improving navigation capabilities in GPS-denied environments through multi-sensor fusion approaches. Regarding datasets, establishing standardized annotation criteria, developing automatic annotation tools, and employing synthetic data generation and domain adaptive strategy can significantly enhance data quality and diversity. For DL algorithms, implementing multi-source data fusion, developing multi-scale feature extraction approaches, and designing lightweight algorithms specifically optimized for edge deployment can improve detection accuracy, generalization capability, and real-time performance.

The integration of these advancements holds potential for infrastructure maintenance and safety management. Beyond defect detection, future systems may evolve toward comprehensive structural health monitoring that combines detection with severity assessment, progress

tracking, and predictive maintenance recommendations. As interdisciplinary collaboration intensifies between civil engineering, computer science, and robotics, the practical implementation of these technologies promises not only reduced inspection costs but also significant impact through enhanced infrastructure safety and resilience. By addressing the current-existing challenges, the greater potential of UAV-based deep learning applications for infrastructure inspection would contribute to a safer and more sustainable infrastructure management system.

CRediT authorship contribution statement

Chen Lyu: Writing – review & editing, Writing – original draft, Visualization, Methodology, Formal analysis, Conceptualization. **Shaoqian Lin:** Writing – review & editing, Visualization. **Angus Lynch:** Writing – review & editing, Visualization. **Yang Zou:** Writing – review & editing. **Minas Liarokapis:** Writing – review & editing, Supervision.

Declaration of competing interest

The authors declare that they have no known competing financial interests or personal relationships that could have appeared to influence the work reported in this paper.

Appendix A

Related papers for statistics are included on the website as supplementary references. The link of the website is as follows: URL: <https://newdexterity.org/uavdlinspectioninfrastructure>

Data availability

No data was used for the research described in the article.

References

- [1] I.O. Agyemang, X. Zhang, I. Adjei-Mensah, D. Acheampong, L.D. Fiasam, C. Sey, S.B. Yussif, D. Effah, Automated vision-based structural health inspection and assessment for post-construction civil infrastructure, *Autom. Constr.* 156 (2023) 105153, <https://doi.org/10.1016/j.autcon.2023.105153>.
- [2] X. Yang, E. del Rey Castillo, Y. Zou, L. Wotherspoon, UAV-deployed deep learning network for real-time multi-class damage detection using model quantization techniques, *Autom. Constr.* 159 (2024) 105254, <https://doi.org/10.1016/j.autcon.2023.105254>.
- [3] G.M. Calvi, M. Moratti, G.J. O'Reilly, N. Scattarreggia, R. Monteiro, D. Malomo, P.M. Calvi, R. Pinho, Once upon a time in Italy: the tale of the Morandi bridge, *Struct. Eng. Int.* 29 (2) (2019) 198–217, <https://doi.org/10.1080/10168664.2018.1558033>.
- [4] E. Jeong, J. Seo, J.P. Wacker, UAV-aided bridge inspection protocol through machine learning with improved visibility images, *Expert Syst. Appl.* 197 (2022) 116791, <https://doi.org/10.1016/j.eswa.2022.116791>.
- [5] E. Khankeshzadeh, A. Mohammadzadeh, H. Arefi, A. Mohsenifar, S. Pirasteh, E. Fan, H. Li, J. Li, A novel weighted ensemble transferred U-net based model (WETUM) for postearthquake building damage assessment from UAV data: A comparison of deep learning-and machine learning-based approaches, *IEEE Trans. Geosci. Remote Sens.* 62 (2024) 1–17, <https://doi.org/10.1109/tgrs.2024.3354737>.
- [6] R. Jiao, Z. Fu, Y. Liu, Y. Zhang, Y. Song, A defective bolt detection model with attention-based RoI fusion and cascaded classification network, *IEEE Trans. Instrum. Meas.* (2023), <https://doi.org/10.1109/tim.2023.3318688>.
- [7] A. Krizhevsky, I. Sutskever, G.E. Hinton, Imagenet classification with deep convolutional neural networks, in: *Advances in Neural Information Processing Systems* 25, 2012, <https://doi.org/10.1145/3065386>.
- [8] J. Redmon, S. Divvala, R. Girshick, A. Farhadi, You only look once: Unified, real-time object detection, *Proc. IEEE Conf. Comp. Vision Pattern Recognition (CVPR)* (2016) 779–788, <https://doi.org/10.1109/cvpr.2016.91>.
- [9] H.-J. Woo, W.-H. Hong, J. Oh, S.-C. Baek, Defining structural cracks in exterior walls of concrete buildings using an unmanned aerial vehicle, *Drones* 7 (3) (2023) 149, <https://doi.org/10.3390/drones7030149>.
- [10] R. Zhang, G. Hao, K. Zhang, Z. Li, Unmanned aerial vehicle navigation in underground structure inspection: A review, *Geol. J.* 58 (6) (2023) 2454–2472, <https://doi.org/10.1002/gj.4763>.
- [11] T.-C. Huynh, J.-H. Park, H.-J. Jung, J.-T. Kim, Quasi-autonomous bolt-loosening detection method using vision-based deep learning and image processing, *Automation Construct.* 105 (2019) 102844, <https://doi.org/10.1016/j.autcon.2019.102844>.

- [12] P. Sharma, S. Saurav, S. Singh, Object detection in power line infrastructure: A review of the challenges and solutions, *Eng. Appl. Artif. Intell.* 130 (2024) 107781, <https://doi.org/10.1016/j.engappai.2023.107781>.
- [13] M. Manjusha, V. Sunitha, A review of advanced pavement distress evaluation techniques using unmanned aerial vehicles, *Int. J. Pavement Eng.* 24 (2) (2023) 2268796, <https://doi.org/10.1080/10298436.2023.2268796>.
- [14] Z. Yahya, S. Imane, H. Hicham, A. Ghassane, E.B.-I. Safia, Applied imagery pattern recognition for photovoltaic modules' inspection: A review on methods, challenges and future development, *Sustain. Energy Technol. Assess.* 52 (2022) 102071, <https://doi.org/10.1016/j.seta.2022.102071>.
- [15] E. Jeong, J. Seo, J. Wacker, Literature review and technical survey on bridge inspection using unmanned aerial vehicles, *J. Perform. Constr. Facil.* 34 (6) (2020) 04020113, [https://doi.org/10.1061/\(ASCE\)CF.1943-5509.0001519](https://doi.org/10.1061/(ASCE)CF.1943-5509.0001519).
- [16] E. Ranyal, A. Sadhu, K. Jain, Road condition monitoring using smart sensing and artificial intelligence: A review, *Sensors* 22 (8) (2022) 3044, <https://doi.org/10.3390/s22083044>.
- [17] M. Azimi, A.D. Eslamloo, G. Pekcan, Data-driven structural health monitoring and damage detection through deep learning: state-of-the-art review, *Sensors* 20 (10) (2020) 2778, <https://doi.org/10.3390/s20102778>.
- [18] C. Ferraris, G. Amprimo, G. Pettiti, Computer vision and image processing in structural health monitoring: overview of recent applications, *Signals* 4 (3) (2023) 539–574, <https://doi.org/10.3390/signals4030029>.
- [19] Y.-J. Cha, R. Ali, J. Lewis, O. Büyükköprü, Deep learning-based structural health monitoring, *Automation Construct.* 161 (2024) 105328, <https://doi.org/10.1016/j.autcon.2024.105328>.
- [20] M.J. Page, J.E. McKenzie, P.M. Bossuyt, I. Boutron, T.C. Hoffmann, C.D. Mulrow, L. Shamseer, J.M. Tetzlaff, E.A. Akl, S.E. Brennan, et al., The PRISMA 2020 statement: an updated guideline for reporting systematic reviews, *Int. J. Surg.* 88 (2021) 105906, <https://doi.org/10.1136/bmj.n71>.
- [21] X. Hu, R.H. Assaad, The use of unmanned ground vehicles (mobile robots) and unmanned aerial vehicles (drones) in the civil infrastructure asset management sector: applications, robotic platforms, sensors, and algorithms, *Expert Syst. Appl.* 232 (2023) 120897, <https://doi.org/10.1016/j.eswa.2023.120897>.
- [22] D.K. Singh, V. Hoskere, Post disaster damage assessment using ultra-high-resolution aerial imagery with semi-supervised transformers, *Sensors* 23 (19) (2023) 8235, <https://doi.org/10.3390/s23198235>.
- [23] S. Tilon, F. Nix, G. Vosselman, I. Sevilla de la Llave, N. Kerle, Towards improved unmanned aerial vehicle edge intelligence: A road infrastructure monitoring case study, *Remote Sensing* 14 (16) (2022) 4008, <https://doi.org/10.3390/rs14164008>.
- [24] P. Aela, H.-L. Chi, A. Fares, T. Zayed, M. Kim, UAV-based studies in railway infrastructure monitoring, *Automation Construct.* 167 (2024) 105714, <https://doi.org/10.1016/j.autcon.2024.105714>.
- [25] Q. Zhang, S.H. Ro, Z. Wan, S. Babanajad, J. Braley, K. Barri, A.H. Alavi, Automated unmanned aerial vehicle-based bridge deck delamination detection and quantification, *Transp. Res. Rec.* 2677 (8) (2023) 24–36, <https://doi.org/10.1177/03611981231155423>.
- [26] J. Zhu, J. Zhong, T. Ma, X. Huang, W. Zhang, Y. Zhou, Pavement distress detection using convolutional neural networks with images captured via UAV, *Autom. Constr.* 133 (2022) 103991, <https://doi.org/10.1016/j.autcon.2021.103991>.
- [27] P. Kumar, S. Batchu, S.R. Kota, et al., Real-time concrete damage detection using deep learning for high rise structures, *IEEE Access* 9 (2021) 112312–112331, <https://doi.org/10.1109/access.2021.3102647>.
- [28] K. Jang, T. Song, D. Kim, J. Kim, B. Koo, M. Nam, K. Kwak, J. Lee, M. Chung, Analytical method for bridge damage using deep learning-based image analysis technology, *Appl. Sci.* 13 (21) (2023) 11800, <https://doi.org/10.3390/app132111800>.
- [29] J.H. Lee, S. Yoon, B. Kim, G.-H. Gwon, I.-H. Kim, H.-J. Jung, A new image-quality evaluating and enhancing methodology for bridge inspection using an unmanned aerial vehicle, *Smart Struct. Syst.* 27 (2) (2021) 209–226, <https://doi.org/10.12989/ss.2021.27.2.209>.
- [30] N. Takhtekeshha, A. Mohammadzadeh, B. Salehi, A rapid self-supervised deep-learning-based method for post-earthquake damage detection using UAV data (case study: Sarpol-e Zahab, Iran), *Remote Sensing* 15 (1) (2022) 123, <https://doi.org/10.3390/rs15010123>.
- [31] C. Xiong, Q. Li, X. Lu, Automated regional seismic damage assessment of buildings using an unmanned aerial vehicle and a convolutional neural network, *Automation Construct.* 109 (2020) 102994, <https://doi.org/10.1016/j.autcon.2019.102994>.
- [32] L.A. Silva, V.R.Q. Leithardt, V.F.L. Batista, G.V. González, J.F.D.P. Santana, Automated Road Damage Detection Using UAV Images and Deep Learning Techniques, In, *IEEE Access*, 2023, <https://doi.org/10.1109/access.2023.3287770>.
- [33] L.A. Silva, H. Sanchez San Blas, D. Peral García, A. Sales Mendes & G. Villarrubia González,, An architectural multi-agent system for a pavement monitoring system with pothole recognition in UAV images, *Sensors* 20 (21) (2020) 6205, <https://doi.org/10.3390/s20216205>.
- [34] G.E. Amieghamen, M.M. Sherif, Deep convolutional neural network ensemble for pavement crack detection using high elevation UAV images, *Struct. Infrastruct. Eng.* (2023) 1–16, <https://doi.org/10.1080/15732479.2023.2263441>.
- [35] F. Nex, D. Duarte, F.G. Tonolo, N. Kerle, Structural building damage detection with deep learning: assessment of a state-of-the-art CNN in operational conditions, *Remote Sensing* 11 (23) (2019) 2765, <https://doi.org/10.3390/rs11232765>.
- [36] C.-F.J. Kuo, S.-H. Chen, C.-Y. Huang, Automatic detection, classification and localization of defects in large photovoltaic plants using unmanned aerial vehicles (UAV) based infrared (IR) and RGB imaging, *Energy Convers. Manag.* 276 (2023) 116495, <https://doi.org/10.1016/j.enconman.2022.116495>.
- [37] Y. Zefri, I. Sebari, H. Hajji, G. Aniba, Developing a deep learning-based layer-3 solution for thermal infrared large-scale photovoltaic module inspection from orthorectified big UAV imagery data, *Int. J. Appl. Earth Obs. Geoinf.* 106 (2022) 102652, <https://doi.org/10.1016/j.jag.2021.102652>.
- [38] S. Dabewtar, R. Padhye, N.N. Kularki, C. Niezrecki, A. Sabato, Performance evaluation of deep learning algorithms for heat loss damage classification in buildings from UAV-borne infrared images, *J. Build. Eng.* 75 (2023) 106948, <https://doi.org/10.1016/j.jobe.2023.106948>.
- [39] W. Tang, Q. Yang, X. Hu, W. Yan, Edge intelligence for smart EL images defects detection of PV plants in the IoT-based inspection system, *IEEE Internet Things J.* 10 (4) (2022) 3047–3056, <https://doi.org/10.1109/iot.2022.3150298>.
- [40] X. Huang, Y. Wu, Y. Zhang, B. Li, Structural defect detection technology of transmission line damper based on UAV image, *IEEE Trans. Instrum. Meas.* 72 (2022) 1–14, <https://doi.org/10.1109/tim.2022.3228008>.
- [41] F. Ni, Z. He, S. Jiang, W. Wang, J. Zhang, A generative adversarial learning strategy for enhanced lightweight crack delineation networks, *Adv. Eng. Inform.* 52 (2022) 101575, <https://doi.org/10.1016/j.aei.2022.101575>.
- [42] Y.Z. Ayele, M. Aliyari, D. Griffiths, E.L. Drogue, Automatic crack segmentation for UAV-assisted bridge inspection, *Energies* 13 (23) (2020) 6250, <https://doi.org/10.3390/en13236250>.
- [43] H.S. Munawar, F. Ullah, D. Shahzad, A. Heravi, S. Qayyum, J. Akram, Civil infrastructure damage and corrosion detection: An application of machine learning, *Buildings* 12 (2) (2022) 156, <https://doi.org/10.3390/buildings12020156>.
- [44] H. Chu, P.-J. Chun, Fine-grained crack segmentation for high-resolution images via a multiscale cascaded network, *Comput. Aided Civ. Inf. Eng.* 39 (4) (2024) 557–594, <https://doi.org/10.1111/mice.13111>.
- [45] J. Yoon, H. Shin, K. Kim, S. Lee, CNN-and UAV-based automatic 3D modeling methods for building exterior inspection, *Buildings* 14 (1) (2023) 5, <https://doi.org/10.3390/buildings14010005>.
- [46] S. Yoon, B.F. Spencer Jr., S. Lee, H.-J. Jung, I.-H. Kim, A novel approach to assess the seismic performance of deteriorated bridge structures by employing UAV-based damage detection, *Struct. Control. Health Monit.* 29 (7) (2022) e2964, <https://doi.org/10.1002/stc.2964>.
- [47] H. Bae, K. Jang, Y.-K. An, Deep super resolution crack network (SrcNet) for improving computer vision-based automated crack detectability in situ bridges, *Struct. Health Monit.* 20 (4) (2021) 1428–1442, <https://doi.org/10.1177/1475921720917227>.
- [48] J. Vazquez-Nicolas, E. Zamora, I. González-Hernández, R. Lozano, H. Sossa, PD+SMC quadrotor control for altitude and crack recognition using deep learning, *Int. J. Control. Autom. Syst.* 18 (4) (2020) 834–844, <https://doi.org/10.1007/s12555-018-0852-9>.
- [49] Y. Zhang, B. Li, J. Shang, X. Huang, P. Zhai, C. Geng, DSA-net: An attention-guided network for real-time defect detection of transmission line dampers applied to UAV inspections, *IEEE Trans. Instrum. Meas.* (2023), <https://doi.org/10.1109/tim.2023.3331418>.
- [50] D. Ma, H. Fang, N. Wang, C. Zhang, J. Dong, H. Hu, Automatic detection and counting system for pavement cracks based on PCGAN and YOLO-MF, *IEEE Trans. Intell. Transp. Syst.* 23 (11) (2022) 22166–22178, <https://doi.org/10.1109/tits.2022.3161960>.
- [51] Y. Feng, S.-J. Feng, X.-L. Zhang, D.-M. Zhang, Y. Zhao, A two-step deep learning-based framework for metro tunnel lining defect recognition, *Tunn. Undergr. Space Technol.* 150 (2024) 105832, <https://doi.org/10.1016/j.tust.2024.105832>.
- [52] N.N. Kularki, K. Raisi, N.A. Valente, J. Benoit, T. Yu, A. Sabato, Deep learning augmented infrared thermography for unmanned aerial vehicles structural health monitoring of roadways, *Autom. Constr.* 148 (2023) 104784, <https://doi.org/10.1016/j.autcon.2023.104784>.
- [53] L. Zhao, H. Zhang, J. Mbachu, Multi-sensor data fusion for 3d reconstruction of complex structures: A case study on a real high formwork project, *Remote Sensing* 15 (5) (2023) 1264, <https://doi.org/10.3390/rs15051264>.
- [54] A. Mirzaade, C. Popescu, J. Gonzalez-Librero, T. Blanksvárd, B. Táljsten, G. Sas, Semi-autonomous inspection for concrete structures using digital models and a hybrid approach based on deep learning and photogrammetry, *J. Civ. Struct. Health Monitor.* 13 (8) (2023) 1633–1652, <https://doi.org/10.1007/s13349-023-00680-x>.
- [55] D. Zhang, R. Watson, G. Dobie, C. MacLeod, G. Pierce, Autonomous ultrasonic inspection using unmanned aerial vehicle, in: 2018 IEEE International Ultrasonics Symposium (IUS), IEEE, 2018, pp. 1–4, <https://doi.org/10.1109/ulstym.2018.8579727>.
- [56] S. Jiang, Y. Cheng, J. Zhang, Vision-guided unmanned aerial system for rapid multiple-type damage detection and localization, *Struct. Health Monit.* 22 (1) (2023) 319–337, <https://doi.org/10.1177/14759217221084878>.
- [57] J. Hou, Y. Yan, P. Cong, Application of technology of UAV-mounted ground penetrating radar in the study of the thickness of soil plow layer, in: IOP Conference Series: Earth and Environmental Science vol. 719, IOP Publishing, 2021, p. 042074, <https://doi.org/10.1088/1755-1315/719/4/042074>, 4.
- [58] R. Salvini, L. Beltramone, V. De Lucia, A. Ermini, C. Vanneschi, C. Zei, D. Silvestri, A. Rindinella, UAV-mounted ground penetrating radar: An example for the stability analysis of a mountain rock debris slope, *J. Mt. Sci.* 20 (10) (2023) 2804–2821, <https://doi.org/10.1007/s11629-023-8162-y>.
- [59] I.O. Agyemang, X. Zhang, D. Acheampong, I. Adjei-Mensah, G.A. Kusi, B. C. Mawuli, B.L.Y. Agbley, Autonomous health assessment of civil infrastructure

- using deep learning and smart devices, *Autom. Constr.* 141 (2022) 104396, <https://doi.org/10.1016/j.autcon.2022.104396>.
- [60] S. Jiang, Y. Wu, J. Zhang, Bridge coating inspection based on two-stage automatic method and collision-tolerant unmanned aerial system, *Autom. Constr.* 146 (2023) 104685, <https://doi.org/10.1016/j.autcon.2022.104685>.
- [61] Y. Jiang, H. Yan, Y. Zhang, K. Wu, R. Liu, C. Lin, RDD-YOLOv5: road defect detection algorithm with self-attention based on unmanned aerial vehicle inspection, *Sensors* 23 (19) (2023) 8241, <https://doi.org/10.3390/s23198241>.
- [62] Y. Zhang, Z. Zuo, X. Xu, J. Wu, J. Zhu, H. Zhang, J. Wang, Y. Tian, Road damage detection using UAV images based on multi-level attention mechanism, *Autom. Constr.* 144 (2022) 104613, <https://doi.org/10.1016/j.autcon.2022.104613>.
- [63] R. Usamentiaga, Semiautonomous pipeline inspection using infrared thermography and unmanned aerial vehicles, *IEEE Trans. Industr. Inform.* 20 (2) (2023) 2540–2550, <https://doi.org/10.2139/ssrn.4415743>.
- [64] Z. Yang, S. Nashik, C. Huang, M. Aibin, L. Coria, Next-gen remote airport maintenance: UAV-guided inspection and maintenance using computer vision, *Drones* 8 (6) (2024) 225, <https://doi.org/10.3390/drones8060225>.
- [65] C. de l'Europe., Eur. Macroseismic Scale 1998 (EMS-98). 15 (1998). Accessed: 2025-5-1. URL: https://www.franceseisme.fr/EMS98_Original_english.pdf.
- [66] Federal Emergency Management Agency (FEMA), Preliminary Damage Assessment Guide, 2024, Accessed: 2025-05-01. URL: <https://www.fema.gov/disaster/how-declared/preliminary-damage-assessments/guide>.
- [67] Federal Emergency Management Agency (FEMA), Hazus hurricane model technical manual, Tech. Rep. 2024. Accessed: 2025-05-30. URL: https://www.fema.gov/sites/default/files/documents/Hazus_6.1_Hurricane_Model_Technical_Manual.pdf.
- [68] C.A. Doswell III, H.E. Brooks, N. Dotzek, On the implementation of the enhanced Fujita scale in the USA, *Atmos. Res.* 93 (1–3) (2009) 554–563, <https://doi.org/10.1016/j.atmosres.2008.11.003>.
- [69] Y. Wang, X. Jing, W. Chen, H. Li, Y. Xu, Q. Zhang, Geometry-informed deep learning-based structural component segmentation of post-earthquake buildings, *Mech. Syst. Signal Process.* 188 (2023) 110028, <https://doi.org/10.1016/j.ymssp.2022.110028>.
- [70] Y. Pi, N.D. Nath, A.H. Behzadan, Convolutional neural networks for object detection in aerial imagery for disaster response and recovery, *Adv. Eng. Inform.* 43 (2020) 101009, <https://doi.org/10.1016/j.aei.2019.101009>.
- [71] Federal Emergency Management Agency (FEMA), Hazus User and Technical Manuals, Accessed: 2025-05-01. URL: <https://www.fema.gov/flood-maps/tools-resources/flood-map-products/hazus/user-technical-manuals>, 2024.
- [72] M. Mundt, S. Majumder, S. Murali, P. Panetos, V. Ramesh, Meta-learning convolutional neural architectures for multi-target concrete defect classification with the concrete defect bridge image dataset, in: Proceedings of the IEEE/CVF Conference on Computer Vision and Pattern Recognition (CVPR), 2019, pp. 11196–11205, <https://doi.org/10.1109/cvpr.2019.01145>.
- [73] Y. Shi, L. Cui, Z. Qi, F. Meng, Z. Chen, Automatic road crack detection using random structured forests, *IEEE Trans. Intell. Transp. Syst.* 17 (12) (2016) 3434–3445, <https://doi.org/10.1109/tits.2016.2552248>.
- [74] Y. Liu, J. Yao, X. Lu, R. Xie, L. Li, DeepCrack: a deep hierarchical feature learning architecture for crack segmentation, *Neurocomputing* 338 (2019) 139–153, <https://doi.org/10.1016/j.neucom.2019.01.036>.
- [75] Q. Zou, Y. Cao, Q. Li, Q. Mao, S. Wang, CrackTree: automatic crack detection from pavement images, *Pattern Recogn. Lett.* 33 (3) (2012) 227–238, <https://doi.org/10.1016/j.patrec.2011.11.004>.
- [76] Q. Zou, Z. Zhang, Q. Li, X. Qi, Q. Wang, S. Wang, Deepcrack: learning hierarchical convolutional features for crack detection, *IEEE Trans. Image Process.* 28 (3) (2018) 1498–1512, <https://doi.org/10.1109/tip.2018.2878966>.
- [77] Y. Narazaki, V. Hoskere, K. Yoshida, B.F. Spencer, Y. Fujino, Synthetic environments for vision-based structural condition assessment of Japanese high-speed railway viaducts, *Mech. Syst. Signal Process.* 160 (2021) 107850, <https://doi.org/10.1016/j.ymssp.2021.107850>.
- [78] F. Yang, L. Zhang, S. Yu, D. Prokhorov, X. Mei, H. Ling, Feature pyramid and hierarchical boosting network for pavement crack detection, *IEEE Trans. Intell. Transp. Syst.* 21 (4) (2019) 1525–1535, <https://doi.org/10.1109/tits.2019.2910595>.
- [79] E. Bianchi, A.L. Abbott, P. Tokek, M. Hebdon, COCO-bridge: structural detail data set for bridge inspections, *J. Comput. Civ. Eng.* 35 (3) (2021) 04021003, [https://doi.org/10.1061/\(asce\)cp.1943-5487.0000949](https://doi.org/10.1061/(asce)cp.1943-5487.0000949).
- [80] M. Eisenbach, R. Stricker, D. Seichter, K. Amende, K. Debes, M. Sesselmann, D. Ebersbach, U. Stoeckert, H.-M. Gross, How to get pavement distress detection ready for deep learning? A systematic approach, in: In: 2017 International Joint Conference on Neural Networks (IJCNN), IEEE, 2017, pp. 2039–2047, <https://doi.org/10.1109/ijcnn.2017.7966101>.
- [81] Ç.F. Özgencil, Concrete Crack Images for Classification. Version V2, Accessed: 2025-05-09. Mendeley Data. URL, <https://data.mendeley.com/datasets/5y9wdsg2zt/2>, 2019.
- [82] M. Maguire, S. Dorafshan, R.J. Thomas, SDNET2018: A Concrete Crack Image Dataset for Machine Learning Applications, Accessed: 2025-05-09, Utah State University, 2018, <https://doi.org/10.15142/T3TD19>. URL
- [83] E. Ichi, F. Jafari, S. Dorafshan, SDNET2021: annotated NDE dataset for subsurface structural defects detection in concrete bridge decks, *Infrastructures* 7 (9) (2022) 107, <https://doi.org/10.3390/infrastructures7090107>.
- [84] E. Bianchi, M. Hebdon, Concrete Crack Conglomerate Dataset. Version 1, Accessed: 2025-05-09, University Libraries, Virginia Tech, 2021, <https://doi.org/10.7294/16625056.v1>.
- [85] V. Hoskere, Y. Narazaki, B.F. Spencer Jr., Physics-based graphics models in 3D synthetic environments as autonomous vision-based inspection testbeds, *Sensors* 22 (2) (2022) 532, <https://doi.org/10.3390/s22020532>.
- [86] Y. Gao, K.M. Mosalam, PEER hub ImageNet: A large-scale multiattribute benchmark data set of structural images, *J. Struct. Eng.* 146 (10) (2020) 04020198, [https://doi.org/10.1061/\(ASCE\)ST.1943-541X.0002745](https://doi.org/10.1061/(ASCE)ST.1943-541X.0002745).
- [87] khanhha, Crack segmentation dataset, Accessed: 2025-05-09. URL, https://github.com/khanhha/crack_segmentation, 2025.
- [88] Y. Ren, J. Huang, Z. Hong, W. Lu, J. Yin, L. Zou, X. Shen, Image-based concrete crack detection in tunnels using deep fully convolutional networks, *Constr. Build. Mater.* 234 (2020) 117367, <https://doi.org/10.1016/j.conbuildmat.2019.117367>.
- [89] S. Kulkarni, S. Singh, D. Balakrishnan, S. Sharma, S. Devnuri, S.C.R. Korlapati, CrackSeg9k: A collection and benchmark for crack segmentation datasets and frameworks, in: European Conference on Computer Vision (ECCV), Springer, 2022, pp. 179–195, https://doi.org/10.1007/978-3-031-25082-8_12.
- [90] P. Kulkarni, Insulator Defect Detection, Accessed: 2025-05-09. URL, <https://kaggle.com/competitions/insulator-defect-detection>, 2022.
- [91] I. Nikolov, M. Nielsen, J. Garnaes, C. Madsen, Wind Turbine Blade Surfaces Dataset. Version V1, Accessed: 2025-05-09, URL, <https://data.mendeley.com/datasets/jrmm82m4mv/1>, 2020.
- [92] S. Mehta, A.P. Azad, S.A. Chemmengath, V. Raykar, S. Kalyanaraman, DeepSolarEye: Power loss prediction and weakly supervised soiling localization via fully convolutional networks for solar panels, in: 2018 IEEE Winter Conference on Applications of Computer Vision (WACV), 2018, pp. 333–342, <https://doi.org/10.1109/wacv.2018.00043>.
- [93] R. Pierdicca, M. Paolanti, A. Felicetti, F. Piccinini, P. Zingaretti, Automatic faults detection of photovoltaic farms: solAir, a deep learning-based system for thermal images, *Energies* 13 (24) (2020) 6496, <https://doi.org/10.3390/en13246496>.
- [94] A. Shihavuddin, X. Chen, V. Fedorov, A. Nymark Christensen, N. Andre Brogaard Riis, K. Branner, A. Bjørholm Dahl & R. Reinhold Paulsen., Wind turbine surface damage detection by deep learning aided drone inspection analysis, *Energies* 12 (4) (2019) 676, <https://doi.org/10.3390/en12040676>.
- [95] E. Alfaro-Mejía, H. Loaiza-Correa, E. Franco-Mejía, A.D. Restrepo-Girón, S. E. Nope-Rodríguez, Dataset for recognition of snail trails and hot spot failures in monocrystalline Si solar panels, *Data Brief* 26 (2019) 104441, <https://doi.org/10.1016/j.dib.2019.104441>.
- [96] D. Arya, H. Maeda, S.K. Ghosh, D. Toshniwal, Y. Sekimoto, RDD2022: A multinational image dataset for automatic road damage detection, *Geosci. Data J.* 11 (4) (2024) 846–862, <https://doi.org/10.1002/gdj3.260>.
- [97] Z. Hong, F. Yang, H. Pan, R. Zhou, Y. Zhang, Y. Han, J. Wang, S. Yang, P. Chen, X. Tong, et al., Highway crack segmentation from unmanned aerial vehicle images using deep learning, *IEEE Geosci. Remote Sens. Lett.* 19 (2021) 1–5, <https://doi.org/10.1109/lgrs.2021.3129607>.
- [98] H. Zhang, W. Yang, H. Yu, H. Zhang, G.-S. Xia, PLD-UAV: Power Line Detection in UAV, Accessed: 2025-05-01. URL, <https://snorkerheng.github.io/PLD-UAV/>, 2019.
- [99] L. Hebbache, D. Amirkhani, M.S. Allili, N. Hammouche, J.-F. Lapointe, Leveraging saliency in single-stage multi-label concrete defect detection using unmanned aerial vehicle imagery, *Remote Sensing* 15 (5) (2023) 1218, <https://doi.org/10.3390/rs15051218>.
- [100] S. Zhao, F. Kang, J. Li, Concrete dam damage detection and localisation based on YOLOv5s-HSC and photogrammetric 3D reconstruction, *Automation Construct.* 143 (2022) 104555, <https://doi.org/10.1016/j.autcon.2022.104555>.
- [101] Y. Liu, J.K. Yeoh, D.K. Chua, Deep learning-based enhancement of motion blurred UAV concrete crack images, *J. Comput. Civ. Eng.* 34 (5) (2020) 04020028, [https://doi.org/10.1061/\(asce\)cp.1943-5487.0000907](https://doi.org/10.1061/(asce)cp.1943-5487.0000907).
- [102] D. Sarkar, S.K. Gunturi, Wind turbine blade structural state evaluation by hybrid object detector relying on deep learning models, *J. Ambient Intel. Humanized Comput.* 12 (8) (2021) 8535–8548, <https://doi.org/10.1007/s12652-020-02587-7>.
- [103] M. Flah, A.R. Suleiman, M.L. Nehdi, Classification and quantification of cracks in concrete structures using deep learning image-based techniques, *Cem. Concr. Compos.* 114 (2020) 103781, <https://doi.org/10.1016/j.cemconcomp.2020.103781>.
- [104] T. Said, M. Rashid, Y. Nemoto, S. Tsukamoto, T. Asai, M. Nishio, CNN-based segmentation frameworks for structural component and earthquake damage determinations using UAV images, *Earthq. Eng. Eng. Vib.* 22 (2) (2023) 359–369, <https://doi.org/10.1007/s11803-023-2174-z>.
- [105] C. Liu, H. Sui, S. Zeng, Efficient building damage assessment from post-disaster aerial video using lightweight deep learning models, *Int. J. Remote Sens.* 44 (22) (2023) 6954–6980, <https://doi.org/10.1080/01431161.2023.2277163>.
- [106] S. Jumaboev, D. Jurakuziev, M. Lee, Photovoltaics plant fault detection using deep learning techniques, *Remote Sensing* 14 (15) (2022) 3728, <https://doi.org/10.3390/rs14153728>.
- [107] K. Liu, B.M. Chen, Industrial UAV-based unsupervised domain adaptive crack recognitions: from database towards real-site infrastructural inspections, *IEEE Trans. Ind. Electron.* 70 (9) (2022) 9410–9420, <https://doi.org/10.1109/tie.2022.3204953>.
- [108] R.-Y. Kung, N.-H. Pan, C.C. Wang, P.-C. Lee, Application of deep learning and unmanned aerial vehicle on building maintenance, *Adv. Civil Eng.* 2021 (2021) 1–12, <https://doi.org/10.1155/2021/5598690>.
- [109] G. Yao, W. Sun, Y. Yang, Y. Sun, L. Xu, J. Zhou, Chromatic aberration identification of fair-faced concrete research based on multi-scale lightweight structured data algorithm, *Front. Mater.* 9 (2022) 851555, <https://doi.org/10.3389/fmats.2022.851555>.

- [110] H.S. Munawar, F. Ullah, A. Heravi, M.J. Thaheem, A. Maqsoom, Inspecting buildings using drones and computer vision: A machine learning approach to detect cracks and damages, *Drones* 6 (1) (2021) 5, <https://doi.org/10.3390/drones6010005>.
- [111] N.M. Levine, Y. Narasaki, B.F. Spencer Jr., Development of a building information model-guided post-earthquake building inspection framework using 3D synthetic environments, *Earthq. Eng. Eng. Vib.* 22 (2) (2023) 279–307, <https://doi.org/10.1007/s11803-023-2167-y>.
- [112] O. Ronneberger, P. Fischer, T. Brox, U-net: Convolutional networks for biomedical image segmentation, in: *Medical Image Computing and Computer-assisted Intervention-MICCAI 2015: 18th International Conference*, 2015, pp. 234–241, https://doi.org/10.1007/978-3-319-24574-4_28.
- [113] K. Chen, G. Reichard, X. Xu, A. Akanmu, Automated crack segmentation in close-range building façade inspection images using deep learning techniques, *J. Build. Eng.* 43 (2021) 102913, <https://doi.org/10.1016/j.jobe.2021.102913>.
- [114] L. Zhang, F. Yang, Y.D. Zhang, Y.J. Zhu, Road crack detection using deep convolutional neural network, in: *IEEE International Conference on Image Processing (ICIP)*, IEEE, 2016, pp. 3708–3712, <https://doi.org/10.1109/icip.2016.7533052>.
- [115] A. Kirillov, E. Mintun, N. Ravi, H. Mao, C. Rolland, L. Gustafson, T. Xiao, S. Whitehead, A.C. Berg, W.-Y. Lo, et al., Segment anything, in: *Proceedings of the IEEE/CVF International Conference on Computer Vision (ICCV)*, 2023, pp. 4015–4026, <https://doi.org/10.1109/iccv51070.2023.00371>.
- [116] Y. Tan, G. Li, R. Cai, J. Ma, M. Wang, Mapping and modelling defect data from UAV captured images to BIM for building external wall inspection, *Automation Construct.* 139 (2022) 104284, <https://doi.org/10.1016/j.autcon.2022.104284>.
- [117] E. Antwi-Bekoe, G. Liu, J.-P. Ainam, G. Sun, X.X. Xie, A deep learning approach for insulator instance segmentation and defect detection, *Neural Comput. & Applic.* 34 (9) (2022) 7253–7269, <https://doi.org/10.1007/s00521-021-06792-z>.
- [118] C. Huang, Y. Zhou, X. Xie, Intelligent diagnosis of concrete defects based on improved mask R-CNN, *Appl. Sci.* 14 (10) (2024) 4148, <https://doi.org/10.3390/app14104148>.
- [119] X. Chen, C. Liu, L. Chen, X. Zhu, Y. Zhang, C. Wang, A pavement crack detection and evaluation framework for a UAV inspection system based on deep learning, *Appl. Sci.* 14 (3) (2024) 1157, <https://doi.org/10.3390/app14031157>.
- [120] I.O. Agyemang, L. Zeng, J. Chen, I. Adjei-Mensah, D. Acheampong, Multivisual modality micro drone-based structural damage detection, *Eng. Appl. Artif. Intell.* 133 (2024) 108460, <https://doi.org/10.1016/j.engappai.2024.108460>.
- [121] Z. Hong, C. Yu, Y. Qin, S. Li, H. Xiao, Z. Wang, N. Qiu, FDSP-HRIID: few-shot detector with self-supervised pretraining for high-speed rail infrastructure defects, *IEEE Trans. Instrum. Meas.* (2024), <https://doi.org/10.1109/tim.2024.3369157>.
- [122] A. Shaik, A. Balasundaram, L.S. Kakarla, N. Murugan, Deep learning-based detection and segmentation of damage in solar panels, *Automation* 5 (2) (2024) 128–150, <https://doi.org/10.3390/automation5020009>.
- [123] Z. Wu, Y. Tang, B. Hong, B. Liang, Y. Liu, Enhanced precision in dam crack width measurement leveraging advanced lightweight network identification for pixel-level accuracy, *Int. J. Intell. Syst.* 2023 (1) (2023) 9940881, <https://doi.org/10.1155/2023/9940881>.
- [124] D. Hu, S. Li, J. Du, J. Cai, Automating building damage reconnaissance to optimize drone mission planning for disaster response, *J. Comput. Civ. Eng.* 37 (3) (2023) 04023006, [https://doi.org/10.1061/\(asce\)cp.1943-5487.0001061](https://doi.org/10.1061/(asce)cp.1943-5487.0001061).
- [125] E.U. Rahman, Y. Zhang, S. Ahmad, H.I. Ahmad, S. Jobaer, Autonomous vision-based primary distribution systems porcelain insulators inspection using UAVs, *Sensors* 21 (3) (2021) 974, <https://doi.org/10.3390/s21030974>.
- [126] Z. Yang, W.C. Lee, H.N. Chan, M. Ge, A real-time tunnel surface inspection system using edge-AI on drone, in: *IEEE International Conference on Mechatronics and Automation (ICMA)*, IEEE, 2022, pp. 749–754, <https://doi.org/10.1109/icma54519.2022.9856230>.
- [127] D. Dwivedi, K.V.S.M. Babu, P.K. Yemula, P. Chakraborty, M. Pal, Identification of surface defects on solar pv panels and wind turbine blades using attention based deep learning model, *Eng. Appl. Artif. Intell.* 131 (2024) 107836, <https://doi.org/10.1016/j.engappai.2023.107836>.
- [128] K. Masita, A. Hasan, T. Shongwe, Defects detection on 110 MW AC wind farm's turbine generator blades using drone-based laser and RGB images with res-CNN3 detector, *Appl. Sci.* 13 (24) (2023) 13046, <https://doi.org/10.3390/app132413046>.
- [129] S. Bemposta Rosende, J. Sánchez-Soriano, C.Q. Gómez Muñoz, J. Fernández Andrés, Remote management architecture of UAV fleets for maintenance, surveillance, and security tasks in solar power plants, *Energies* 13 (21) (2020) 5712, <https://doi.org/10.3390/en13215712>.
- [130] A. Mirzazade, C. Popescu, T. Blanksvärd, B. Täljsten, Workflow for off-site bridge inspection using automatic damage detection-case study of the pahtajokk bridge, *Remote Sensing* 13 (14) (2021) 2665, <https://doi.org/10.3390/rs13142665>.
- [131] M.A. Khan, A. Khan, M. Ahmad, S. Saleem, M.S. Aziz, S. Hussain, F.M. Khan, A study on flight time enhancement of unmanned aerial vehicles (UAVs) using supercapacitor-based hybrid electric propulsion system (HEPS), *Arab. J. Sci. Eng.* 46 (2021) 1179–1198, <https://doi.org/10.1007/s13369-020-04941-5>.
- [132] Z. Wang, S. Liu, G. Chen, W. Dong, Robust visual positioning of the UAV for the under bridge inspection with a ground guided vehicle, *IEEE Trans. Instrum. Meas.* 71 (2021) 1–10, <https://doi.org/10.1109/tim.2021.3135544>.
- [133] A. Shihavuddin, M.R.A. Rashid, M.H. Maruf, M.A. Hasan, M. A. ul Haq, R. H. Ashique & A. Al Mansur., Image based surface damage detection of renewable energy installations using a unified deep learning approach, *Energy Rep.* 7 (2021) 4566–4576, <https://doi.org/10.1016/j.egyr.2021.07.045>.
- [134] X.-W. Ye, S.-Y. Ma, Z.-X. Liu, Y. Ding, Z.-X. Li, T. Jin, Post-earthquake damage recognition and condition assessment of bridges using UAV integrated with deep learning approach, *Struct. Control. Health Monit.* 29 (12) (2022) e3128, <https://doi.org/10.1002/stc.3128>.
- [135] M. Żarski, B. Wójcik, J.A. Miszczałk, B. Blachowski, M. Ostrowski, Computer vision based inspection on post-earthquake with UAV synthetic dataset, *IEEE Access* 10 (2022) 108134–108144, <https://doi.org/10.1109/access.2022.3212918>.
- [136] C. Li, S.C. Sun, Z. Wei, A. Tsourdos, W. Guo, Scarce data driven deep learning of drones via generalized data distribution space, *Neural Comput. & Applic.* 35 (20) (2023) 15095–15108, <https://doi.org/10.1007/s00521-023-08522-z>.
- [137] G.-H. Gwon, J.-H. Lee, I.-H. Kim, S.-C. Baek, H.-J. Jung, Image-to-image translation-based structural damage data augmentation for infrastructure inspection using unmanned aerial vehicle, *Drones* 7 (11) (2023) 666, <https://doi.org/10.3390/drones7110666>.
- [138] Y. Li, W. Hu, H. Dong, X. Zhang, Building damage detection from post-event aerial imagery using single shot multibox detector, *Appl. Sci.* 9 (6) (2019) 1128, <https://doi.org/10.3390/app9061128>.
- [139] A. Ratner, S.H. Bach, H. Ehrenberg, J. Fries, S. Wu, C. Ré, Snorkel: Rapid training data creation with weak supervision, in: *Proceedings of the VLDB Endowment. International Conference on Very Large Data Bases* 11, 2017, pp. 269–282, <https://doi.org/10.14778/3157794.3157797>.
- [140] Z.-H. Zhou, A brief introduction to weakly supervised learning, *Nat. Sci. Rev.* 5 (1) (2018) 44–53, <https://doi.org/10.1093/nsr/nwx106>.
- [141] Q. Li, X. Peng, X. Zhong, X. Xiao, H. Wang, C. Zhao, K. Zhou, Quantitative identification of debonding defects in building façades based on UAV-thermography using a two-stage network integrating dual attention mechanism, *Infrared Phys. Technol.* 138 (2024) 105241, <https://doi.org/10.1016/j.infrared.2024.105241>.
- [142] E. Xie, W. Wang, Z. Yu, A. Anandkumar, J.M. Alvarez, P. Luo, SegFormer: simple and efficient design for semantic segmentation with transformers, *Adv. Neural Inf. Proces. Syst.* 34 (2021) 12077–12090, in: https://proceedings.neurips.cc/paper_files/paper/2021/file/64f1f27bf1b4ec22924fd0acb550c235-Paper.pdf.
- [143] S. Mehta, M. Rastegari, Mobilevit: light-weight, general-purpose, and mobile-friendly vision transformer, *arXiv preprint* (2021), <https://doi.org/10.48550/arXiv.2110.02178>.
- [144] A.G. Howard, M. Zhu, B. Chen, D. Kalenichenko, W. Wang, T. Weyand, M. Andreetto, H. Adam, Mobilenets: efficient convolutional neural networks for mobile vision applications, *arXiv preprint* (2017) arXiv:1704.04861. URL <https://arxiv.org/abs/1704.04861>.
- [145] M. Tan, Q. Le, Efficientnet: rethinking model scaling for convolutional neural networks, in: *International Conference on Machine Learning (ICML)*, PMLR, 2019, pp. 6105–6114. URL <https://proceedings.mlr.press/v97/tan19a.html>.
- [146] A.B. Jreddi, A. Shafeeqzadeh, R. Nateghi, PDP-CNN: A deep learning model for post-hurricane reconnaissance of electricity infrastructure on resource-constrained embedded systems at the edge, *IEEE Trans. Instrum. Meas.* 72 (2023) 1–9, <https://doi.org/10.1109/tim.2023.3236321>.